JCI The Journal of Clinical Investigation

Severe peri-ictal respiratory dysfunction is common in Dravet syndrome

YuJaung Kim, … , Douglas R. Nordli Jr., George B. Richerson

J Clin Invest. 2018. https://doi.org/10.1172/JCI94999.

Research Article **Neuroscience**

Dravet syndrome (DS) is a severe childhood-onset epilepsy commonly due to mutations of the sodium channel gene *SCN1A*. DS patients have a high risk of sudden unexplained death in epilepsy (SUDEP), believed to be due to cardiac mechanisms. Here we show that DS patients have peri-ictal respiratory dysfunction. One patient who had severe and prolonged postictal hypoventilation later died of SUDEP. Mice with an $Scn1a^{R1407X/+}$ loss of function mutation died after spontaneous and heat-induced seizures due to central apnea followed by progressive bradycardia. Death could be prevented with mechanical ventilation after seizures induced by hyperthermia or maximal electroshock. Muscarinic receptor antagonists did not prevent bradycardia or death when given at doses selective for peripheral parasympathetic blockade, whereas apnea was prevented at doses known to be high enough to cross the blood brain barrier. Anoxia causes bradycardia due to a direct effect on the heart. We conclude that SUDEP in DS may result in some cases from primary central apnea, which can cause bradycardia presumably via an effect of hypoxemia on cardiac muscle.

Severe Peri-Ictal Respiratory Dysfunction is Common in Dravet Syndrome

*YuJaung Kim[1,2], *Eduardo Bravo[1], Caitlin K. Thirnbeck[1], Lori A. Smith-Mellecker[1], Se Hee Kim[3,♯], Brian K. Gehlbach[4], Linda C. Laux[3], Douglas R. Nordli, Jr.[3,†] & George B. Richerson[1,5,6,§]

Affiliations:

[1]Department of Neurology, University of Iowa, Iowa City, IA

[2]Department of Biomedical Engineering, University of Iowa, Iowa City, IA

[3]Division of Pediatric Neurology, Northwestern University, Chicago, IL

[4]Department of Internal Medicine, University of Iowa, Iowa City, IA

[5]Department of Molecular Physiology & Biophysics, University of Iowa, Iowa City, IA

[6]Neurology, Veterans Affairs Medical Center, Iowa City, IA

[§]Correspondence to: George B. Richerson, 200 Hawkins Drive, Department of Neurology, 2151 RCP, University of Iowa, Iowa City, IA 52242. (319) 353-4400. George-Richerson@UIowa.Edu.

[†]Current Address: Children's Hospital Los Angeles, Keck School of Medicine, University of Southern California, Los Angeles, CA

[♯]Current Address: Division of Pediatric Neurology, Severance Children's Hospital, and Department of Pediatrics, Yonsei University College of Medicine, Seoul, South Korea

*These two authors contributed equally to the work.

Keywords:

Epilepsy / *Scn1a* / SUDEP / Breathing

Footnotes:

Conflict of interest: The authors have declared that no conflict of interest exists.

Abstract: Dravet Syndrome (DS) is a severe childhood-onset epilepsy commonly due to mutations of the sodium channel gene *SCN1A*. DS patients have a high risk of sudden unexplained death in epilepsy (SUDEP), widely believed to be due to cardiac mechanisms. Here we show that DS patients commonly have peri-ictal respiratory dysfunction. One patient had severe and prolonged postictal hypoventilation during video EEG monitoring, and died later of SUDEP. Mice with an *Scn1a*$^{R1407X/+}$ loss of function mutation were monitored, and died after spontaneous and heat-induced seizures due to central apnea followed by progressive bradycardia. Death could be prevented with mechanical ventilation after seizures were induced by hyperthermia or maximal electroshock. Muscarinic receptor antagonists did not prevent bradycardia or death when given at doses selective for peripheral parasympathetic blockade, whereas apnea was prevented by the same drugs given at doses high enough to cross the blood brain barrier. When given via intracerebroventricular infusion at a very low dose, a muscarinic receptor antagonist prevented apnea and death. We conclude that SUDEP in DS results in some cases from primary central apnea, which can cause bradycardia presumably via a direct effect of hypoxemia on cardiac muscle.

Introduction

Patients with epilepsy have a high risk of sudden death (1). The underlying mechanisms of this SUDEP are unknown, but it is believed that most deaths occur immediately after a seizure (2, 3). To identify premorbid biomarkers of patients at highest risk for SUDEP, to develop targeted preventative treatments, and to recommend effective methods for rescuing patients from near-SUDEP, it is necessary to define the sequence of events that leads from a seizure to death.

A variety of mechanisms have been proposed for SUDEP (1, 2, 4-6), including cardiac arrhythmias (7-10), dysfunction of autonomic control (11-15), apnea/hypoventilation (3, 16-21), airway obstruction (22), pulmonary edema (23), brainstem spreading depolarization (BSD) (24) and postictal generalized EEG suppression (PGES) (25). Many investigators have focused on cardiac tachyarrhythmias as the cause of death, in part because of an association between SUDEP and mutations of genes expressed in the heart such as those that underlie long QT syndrome (10, 26-28). In some cases these mutations may cause both arrhythmias and seizures (10, 29, 30), whereas in other cases the mutations may predispose patients to arrhythmias if they have seizures due to other reasons. In epilepsy monitoring unit (EMU) patients, non-fatal seizures can sometimes induce bradycardia, asystole, O_2 desaturation or apnea (4, 5, 8, 16, 17). A small number of patients (n=11) were recently reported who died of SUDEP while being monitored in EMUs (2). In those patients, the typical sequence of events was a generalized tonic-clonic seizure followed by bradycardia and asystole (2), along with decreased respiratory rate leading to terminal apnea. For those patients, measurements were not made of blood pressure, ventilation, CO_2 levels or O_2 saturation, so there are still important unanswered questions about mechanisms, such as whether there was hypotension or if lung inflation was effective. It is also not clear what happened during the seizures, as respiratory movements and the electrocardiogram (EKG) were obscured by convulsive movements. Most of the monitored SUDEP patients had temporal lobe epilepsy, so it is not clear whether those data are relevant to SUDEP in patients with other types of epilepsy. However, all of these SUDEP cases involved terminal apnea first, followed by terminal asystole.

Dravet Syndrome is an intractable epileptic encephalopathy in which febrile seizures typically appear in the first 6-12 months of life, followed by other types of severe, refractory seizures and cognitive impairment (31). In 70-95% of cases, DS is due to mutations of *SCN1A* (32-34), which encodes the sodium channel Nav1.1. SUDEP is particularly common in patients with DS, causing death in 5-10% of cases, most commonly during the first few years of life (31, 35, 36).

Clinical data have pointed to cardiac mechanisms being important for SUDEP in DS. For example, mutations of *SCN1A* in patients with DS cause increased QT and P wave dispersion and a decrease in heart rate variability (HRV) (12, 37). However, there are no published reports of EKG changes after fatal or non-fatal generalized seizures in patients with DS, other than a single case report after status epilepticus (38). Peri-ictal breathing has not been measured in DS patients.

Mouse models of DS have been generated by knockout of *Scn1a*, or with mutations such as R1407X, which is seen in some patients and leads to truncation of Nav1.1 and functional inactivation (39). The phenotype of the $Scn1a^{R1407X/+}$ mutation and the *Scn1a* knockout are similar and recapitulate the phenotype of DS in humans (31), including seizures that occur spontaneously and in response to hyperthermia (7, 39, 40). Heat-induced seizures in DS mice

are often followed by death (7, 40). In addition to the brain, Nav1.1 is expressed in the heart, including the sinoatrial node (41) and cardiac t tubules (42). Mice with an *Scn1a*$^{R1407X/+}$ mutation have cardiac myocyte dysfunction and die spontaneously at a young age after severe bradycardia, which has been interpreted as indicating that these mice die from intrinsic cardiac dysfunction (7). However, selective knockout of *Scn1a* only in brain interneurons results in seizures and spontaneous death (43). In mice with global knockout of *Scn1a*, heat-induced seizures are associated with progressively worsening bradycardia followed by terminal asystole (40). Bradycardia and death can be prevented by pretreatment with atropine (40). These data led to a different conclusion - that death in this mouse model of DS is due to increased vagal output to the heart (40). However, measurements of breathing have not been made during spontaneous or heat-induced seizures in either of these DS mouse models, so it is unclear whether abnormal breathing contributes to SUDEP. Here we studied DS patients and mice with an *Scn1a*$^{R1407X/+}$ mutation (39) to evaluate a potential role of postictal breathing dysfunction in SUDEP.

Results

Peri-ictal respiratory dysfunction was common in DS patients. Video recordings of generalized seizures from seven DS patients and seven patients with localization-related epilepsy were reviewed by an investigator (GBR) blind to the cause of epilepsy. Visualization of chest and abdomen movements, aided by Eulerian video magnification (44), was used to evaluate breathing frequency and pattern (see Methods; Supplemental Figure 1). Patients with DS were significantly more likely to have peri-ictal abnormal breathing consistent with disturbances of respiratory rhythm generation or patterned output (Table 1; p=0.018, Chi-square test), including paradoxical breathing, inspiratory efforts with two or three peaks, ataxic breathing or apnea of 5 s or longer (Figure 1; Supplemental Figure 2; Supplemental Video 1 & 2). Many patients produced loud upper airway sounds consistent with obstruction, but this was not significantly more common in either group (Table 1). In all of these cases, breathing abnormalities were transient.

Video recordings can reveal valuable information about peri-ictal respiratory patterns, but as was true for previously reported EMU recordings (2), this approach leaves many unanswered questions (see Introduction). To more accurately characterize abnormalities of peri-ictal breathing, a nine year old girl with DS and an associated de novo missense mutation of *SCN1A* was admitted for recording of video-EEG, which was supplemented with recordings of respiratory impedance plethysmography (RIP), and transcutaneous CO_2 ($tcCO_2$) (Figure 2). The patient had three consecutive generalized tonic-clonic seizures. The seizures on EEG lasted 48, 89 and 90 s, separated by 1-3 minutes (Figure 2A). Rectal diazepam (0.5 mg/kg) was given during the second seizure. Between seizures the patient's eyes were open but she had a limited response to verbal and tactile stimuli, and the EEG showed continuous slowing with frequent interictal epileptiform discharges. Epileptiform discharges and EEG slowing decreased after the third seizure.

Before the first seizure, plethysmography revealed normal, regular breathing (Figure 2B), and $tcCO_2$ was 44 mmHg. During and after the seizures she developed labored breathing with periods of apnea lasting up to 13 seconds (Figure 2C-E). After the first seizure, oxygen desaturation occurred and the patient was treated with O_2 delivered by a non-rebreather mask at an initial rate of 15 LPM and subsequently adjusted to keep O_2 saturation > 92%. O_2 was

removed after the 3rd seizure. $tcCO_2$ increased during the seizures to 53-55 mmHg. Approximately 45 minutes after the third seizure the patient developed labored breathing. Oxygen desaturation occurred and O_2 was given again. At the time, $tcCO_2$ had increased to 68 mmHg and remained at 70 mmHg for the next hour. At two hours, a painful stimulus was given that caused the patient to arouse, and $tcCO_2$ declined to just above 50 mmHg where it remained for an additional 2 hours before returning to baseline. During most of the time after the seizures the patient continued breathing at a rate of 18-22 without apnea (Figure 2E). However, the elevated $tcCO_2$ indicated there was marked hypoventilation - apparently due to decreased tidal volume. It is not clear whether diazepam contributed to the hypoventilation. This case was remarkable for impairment of respiratory CO_2 chemoreception that continued long after the seizure. It also demonstrates that supplementary oxygen is not adequate treatment when the primary problem is hypoventilation. Three years after this recording, the patient was found face down in bed, was blue and pulseless, and could not be resuscitated. An autopsy was performed and the cause of death was given as SUDEP.

Taken together, these data indicate that many patients with DS have peri-ictal respiratory dysfunction that can extend long into the postictal period, including defects in respiratory rhythm generation, impaired central CO_2 chemoreception, and loss of airway patency. In the non-fatal episodes documented here, these changes were transient, but the severe defects in breathing in the patient who later died of SUDEP suggest that respiratory changes may be biomarkers of patients at high risk.

Spontaneous seizures caused death in *Scn1a*$^{R1407X/+}$ mice due to respiratory arrest. Heterozygous *Scn1a*$^{R1407X/+}$ knock-in mice, that express a mutation described in three unrelated DS patients, were used to define the cause of death after seizures (39). Video recordings were made continuously from 78 *Scn1a*$^{R1407X/+}$ mice between the ages of 16 days postnatal (P16) and P60. During that time, 38% of the mice spontaneously died (n=30 of 78) (Figure 3). There was no difference in mortality between male and female mice (Supplemental Figure 3). Review of the video recordings revealed that all spontaneous deaths occurred after a generalized seizure characterized by tonic hindlimb extension. All spontaneous seizures with tonic hindlimb extension were fatal.

To better understand the cause of postictal death in *Scn1a*$^{R1407X/+}$ mice than is possible using video recording alone, a custom-designed mouse EMU was used to continuously monitor EEG, EKG, EMG, video and plethysmography. From 4680 hours of recording from 19 *Scn1a*$^{R1407X/+}$ mice, two mice died from spontaneous seizures. In one mouse that was monitored for 408 hours from P23 to P40 (Figure 4), death occurred after a seizure with tonic hindlimb extension. Breathing and heart rate were both normal prior to the seizure. During the seizure, the mouse suddenly developed complete apnea that continued into the postictal period and never recovered. There was also a rapid decrease in heart rate shortly after the onset of apnea, but the heartbeat remained above 25-51% of control for 60 seconds after the onset of apnea, and continued for almost four minutes after the end of the seizure with slowly worsening bradycardia eventually leading to terminal asystole. A similar sequence of events was seen in a second mouse monitored for 33 hours starting at P23 (Supplemental Figure 4). These observations suggest that respiratory arrest played a key role in death of these animals. For both mice, recordings revealed central apnea, as there was no evidence for airway obstruction in the video recording, EMG or plethysmography trace. Notably, the EEG rapidly became flat after the seizure, consistent with PGES (25). This same observation was reported previously after

maximal electroshock (MES) induced seizures in *Lmx1b*$^{f/f/p}$ mice, which lack over 99% of 5-HT neurons in the CNS (19).

Auerbach et al (7) reported episodes of bradycardia and increased HRV in *Scn1a*$^{R1407X/+}$ mice up to 48 hours prior to death. They did not measure breathing or EEG during those episodes, so it is not known if the bradycardia occurred during seizures or was accompanied by apnea. During our experiments we measured the EEG and breathing, along with the EKG, so were able to evaluate whether spontaneous episodes of bradycardia were due to seizures or apnea. During a total of 441 hours monitoring EEG, EKG and plethysmography from the two mice that died spontaneously, one had three spontaneous non-fatal seizures and the other had four. All seven of these seizures were generalized with clonic limb contractions, and were classified as Racine scale 5 seizures. Three of these non-fatal seizures included transient episodes of apnea and bradycardia that were less severe than during fatal seizures (Supplemental Figure 5). Bradycardia never occurred without apnea or severely decreased breath amplitude.

Heat-induced seizures also caused respiratory arrest in *Scn1a*$^{R1407X/+}$ mice. As in DS patients (31), an increase in body temperature can induce seizures in *Scn1a*$^{R1407X/+}$ mice (45) and *Scn1a* knockout mice (40). It has been reported that heat-induced seizures in DS mice lead to bradycardia followed by death (40). Here we verified that a rise in body temperature induced seizures in *Scn1a*$^{R1407X/+}$ mice, with the first seizure occurring at an average of 39.67±0.97 degrees C (n=21) leading to death in 18 of 21 mice after 3.53±0.68 seizures. As reported previously with fatal heat-induced seizures in *Scn1a* knockout mice (40), electrographic seizures accompanied by tonic hindlimb extension or clonic limb contractions were followed by a decrease in heart rate that eventually resulted in terminal asystole (Supplemental Figure 6). However, we found that fatal seizures also always involved terminal apnea. This apnea occurred precipitously during the seizure or within seconds of the end of the seizure. In contrast, mild to moderate bradycardia often occurred shortly after the onset of apnea, but a heartbeat continued, slowly decreasing over time with terminal asystole not occurring until 3.89 ± 0.92 minutes after the end of seizures. Death could be prevented if mechanical ventilation was initiated within 5-10 seconds of the onset of apnea using a rodent ventilator (MiniVent type 845; Harvard Apparatus, Holliston, MA) connected to plastic tubing placed over the mouse's nostrils (n=5 mice). Death in this group of mice always occurred due to apnea, and bradycardia only occurred if there was apnea.

MES also induced generalized seizures in *Scn1a*$^{R1407X/+}$ mice, but these seizures were less likely to cause apnea (four episodes of apnea after seizures in 34 mice). When apnea did occur, death was prevented by mechanical ventilation in three of four mice.

High dose atropine prevented peri-ictal apnea in *Scn1a*$^{R1407X/+}$ mice. It has previously been shown that atropine prevents postictal bradycardia and death in *Scn1a* knockout mice after hyperthermia-induced seizures (40). This led to the conclusion that seizures cause fatal bradycardia due to an increase in vagal parasympathetic output and activation of cardiac muscarinic acetylcholine receptors (40). To examine the mechanism by which atropine prevents postictal death, we induced seizures in *Scn1a*$^{R1407X/+}$ mice with hyperthermia 30 minutes after pretreatment with 1 mg/kg (i.p.) atropine, and compared the seizures to a matched cohort of *Scn1a*$^{R1407X/+}$ mice. Atropine (1 mg/kg) did not reduce the likelihood of Racine scale 5 seizures, or the duration or severity of seizures as determined by EEG analysis (See Methods), but did

reduce the likelihood of tonic hindlimb extension. Death occurred in seven of nine mice treated with atropine (1 mg/kg) compared to zero of six mice treated with vehicle (Figure 5A). Unexpectedly, atropine (1 mg/kg) also prevented apnea in all mice that survived (n=7/9) (Figure 5B). For mice treated with atropine that died (n=2/9), the sequence of events was identical to that of mice treated with vehicle, with immediate and complete apnea beginning near the end of a generalized seizure, followed by slowly progressive bradycardia.

It is common to use atropine at a dose of 1 mg/kg to block peripheral muscarinic receptors in rodents. However, that dose is 20-50 times higher than is recommended for specific blockade of peripheral muscarinic receptors in mice (0.02-0.05 mg/kg i.p.) (46-48). Atropine can readily cross the blood brain barrier (49, 50). After 30 minutes CNS levels reach more than 35% of serum levels (49). After a dose of 1 mg/kg this would be more than enough to block central muscarinic receptors. Muscarinic acetylcholine receptors in the medulla and pons play an important role in respiratory control (51, 52) and central CO_2 chemoreception (53, 54), and those in the forebrain alter seizure activity (55).

Quaternary ammonium derivatives of muscarinic receptor antagonists, such as methylatropine and N-methylscopolamine, are used as selective antagonists of peripheral muscarinic receptors, as they are less likely to penetrate the blood brain barrier (56, 57). N-methylscopolamine (1 mg/kg; i.p.) has previously been shown to prevent bradycardia and death after heat-induced seizures in *Scn1a* knockout mice, supporting the hypothesis that postictal bradycardia is due to an increase in vagal tone (40). We replicated this experiment in *Scn1a*$^{R1407X/+}$ mice (n=6), but found that pretreatment with N-methylscopolamine (1 mg/kg; i.p.) 30 minutes prior to inducing seizures with hyperthermia did not prevent apnea, bradycardia or death (Figure 5A). In contrast, methylatropine (1 mg/kg; i.p.) (n=6) did prevent bradycardia and death (Figure 5A), but also prevented apnea (as in Figure 5B). Selective blockade of peripheral muscarinic receptors would not be expected to prevent apnea, because the neural circuitry involved in generation of respiratory output is contained entirely within the CNS, as are descending projections from the forebrain that cause apnea during and/or after seizures (18, 20). Instead, the effect of methylatropine is likely to be due to penetration into the CNS. After equivalent doses of radioactive atropine or methylatropine, both drugs accumulate in the CNS (58). Systemic methylatropine has effects on cortical activity that are dependent on the dose and treatment duration, with 1 mg/kg (i.v.) inhibiting EEG activity by 70% within 20-30 minutes (59). Thus, at high doses quaternary ammonium anticholinergic agents can have central effects that are protective against apnea.

Selective blockade of peripheral muscarinic receptors does not prevent postictal bradycardia. A dose of atropine of 0.02-0.04 mg/kg (i.p.) is recommended to block peripheral parasympathetic activity in mice (46-48). Measurement of HRV can be used to determine whether muscarinic receptor antagonists are effective at blocking vagal parasympathetic output to the heart. The most common type of HRV, respiratory sinus arrhythmia, is due to changes in parasympathetic output caused by breathing (60-64). This results in part from an increase in intrathoracic pressure during expiration, which leads to an increase in systemic blood pressure and reflex bradycardia (and opposite changes during inspiration). Blocking parasympathetic output eliminates this form of HRV (60-64). To verify that muscarinic receptor antagonists were effective in blocking peripheral muscarinic receptors, Poincaré plots were used to analyze variability of the R-R interval on the EKG (Figure 6). Compared to WT mice, *Scn1a*$^{R1407X/+}$ mice had significantly greater long-term (SD2) HRV (Figure 6A-B; Supplemental Figure 7C-D).

Atropine reduced long-term HRV (SD2) in *Scn1a*$^{R1407X/+}$ mice, and was equally effective at 1 mg/kg and 0.03 mg/kg (Figure 6C-D; Supplemental Figure 7C-D). Despite the ability of the lower dose of atropine to block peripheral muscarinic receptors, all *Scn1a*$^{R1407X/+}$ mice in which seizures with tonic hindlimb extension were induced by hyperthermia after pretreatment with 0.03 mg/kg atropine still developed bradycardia and died (Figure 5A; n = 6 of 6), but they also developed apnea (data not shown). N-methylscopolamine (1 mg/kg; n=6) and methylatropine (1 mg/kg; n=6) both caused a decrease in short-term (SD1) and long-term HRV (SD2) (Supplemental Figure 7). Despite the ability of all of these treatments to block vagal parasympathetic output, only some prevented postictal bradycardia and death. Those treatments that were protective prevented peri-ictal apnea, and those that were not protective did not prevent apnea.

Selective blockade of central muscarinic receptors prevented peri-ictal apnea and bradycardia. *Scn1a*$^{R1407X/+}$ mice (n=5) were treated with intracerebroventricular (i.c.v.) N-methylscopolamine at a dose of only (0.3 μg/kg) . This agent was the least permeable across the blood brain barrier (see above), so it should have remained restricted to the CNS. However, even if the drug freely crossed the BBB and distributed throughout the body this dose would still be only 1% of that required to block peripheral muscarinic receptors (0.03 mg/kg), and thus would not reach levels high enough to block parasympathetic drive to the heart. Thirty minutes after i.c.v. injection of N-methylscopolamine (0.3 μg/kg), hyperthermia was induced to at least 42.5 ºC, resulting in an average of 3.33±0.89 seizures per mouse. Generalized seizures were induced in 5 of 5 mice at a body temperature of 40.7±0.53 ºC. All of the *Scn1a*$^{R1407X/+}$ mice had generalized seizures with tonic hindlimb extension or clonic limb contractions (n=5), but none developed apnea, bradycardia, or death (Figure 7A). Poincaré plots were used to evaluate EKG changes. There was no change in mean heart rate or HRV after i.c.v. N-methylscopolamine (0.3 μg/kg) (Figure 7B). Thus, i.c.v. N-methylscopolamine had no effect on peripheral muscarinic receptors, but prevented bradycardia by blocking apnea via an effect in the CNS.

Hypoxia caused bradycardia due to a direct effect on the heart. Based on the above results, we hypothesized that seizures caused apnea, and the resulting hypoxia had a direct negative chronotropic effect on cardiac tissue. Consistent with this possibility, during vascular perfusion of the isolated rat heart *ex vivo* it has been shown that hypoxia causes a decrease in heart rate and cardiac contractility due to a direct effect on the heart (66). WT (n=5) and *Scn1a*$^{R1407X/+}$ (n=6) mice were anesthetized with isoflurane (1%) and placed in a whole body plethysmograph. After recording baseline EKG and breathing, ambient gas was switched from normoxia (21% O_2/79% N_2) to anoxia (0% O_2/100% N_2). This led to bradycardia with a time course similar to that seen after seizures in *Scn1a*$^{R1407X/+}$ mice (Figure 8). It also caused a decrease in amplitude of the QRS complex, as also occurred after fatal seizures - presumably a surrogate of decreased cardiac contractility (66). Pretreatment of WT mice with atropine at 1 mg/kg (n=5) did not prevent the bradycardia induced by anoxia (Figure 8), indicating that the decrease in heart rate was not mediated by an increase in vagal output.

Discussion

Here we show that patients with DS have peri-ictal breathing dysfunction, including ataxic respiratory output, paradoxical breathing, airway obstruction and prolonged depression of CO_2 chemoreception that lasted as long as 4 hours after the end of seizures. The respiratory

abnormalities we recorded were transient. However, a child with particularly severe and prolonged postictal hypoventilation later died of SUDEP. These results suggest that postictal ventilatory abnormalities may play a major role in SUDEP in patients with DS, and may be a biomarker for those at highest risk.

We also studied seizures in a mouse model of DS, and found that postictal death was due to immediate fatal apnea. In contrast, Kalume et al (40) reported that postictal death after heat-induced seizures in *Scn1a* knockout mice is due to severe bradycardia and this was proposed to be due to increased vagal parasympathetic tone. This conclusion was supported by data showing that death was prevented by treatment with atropine (40). Auerbach et al (7) reported spontaneous death preceded by bradycardia in three $Scn1a^{R1407X/+}$ mice, and in that case death was attributed to abnormal intrinsic electrophysiological properties of cardiac myocytes (7). However, breathing was not measured in either of those studies. Here we report postictal bradycardia in $Scn1a^{R1407X/+}$ mice with a similar time course as that reported in those other studies (7, 40), but found that central apnea occurred prior to bradycardia. Apnea rapidly causes hypoxemia in mice and rats within seconds (67, 68). Therefore, the long duration of apnea we saw in response to seizures would be expected to cause a severe drop in blood oxygen. Hypoxemia has a negative chronotropic effect on the heart (66), explaining why atropine did not prevent bradycardia in response to exposure to hypoxic gas (Figure 8).

We found that atropine was protective against peri-ictal bradycardia, but this was not due to blockade of parasympathetic output. Instead, at high doses atropine prevented peri-ictal apnea due to a central effect. Peri-ictal apnea and bradycardia were not prevented by selective blockade of peripheral muscarinic receptors using atropine at a low dose (0.03 mg/kg i.p.), or the relatively membrane impermeable N-methylscopolamine at high dose (1 mg/kg i.p.). In both cases, blockade of peripheral muscarinic receptors was verified by suppression of HRV. In contrast, peri-ictal apnea and bradycardia were both prevented by selective blockade of central muscarinic receptors using very low dose N-methylscopolamine (0.3 μg/kg) administered i.c.v. Mice were protected from death even though peripheral muscarinic receptors were not blocked, as verified by a lack of effect on HRV. These results indicate that atropine prevents postictal death by blocking central apnea rather than blocking vagal output.

Our results with systemic N-methylscopolamine were different from those of Kalume et al (40), who found protection from death despite using the same concentration and route of delivery. The reason for this difference is unclear, but it is possible that the drug was able to penetrate into the CNS more easily in their study, such as if the blood brain barrier was leakier due to a larger number of seizures. There may also be strain differences in sensitivity to the drug. Although relatively membrane impermeable, N-methylscopolamine can still cross the blood brain barrier. However, given its equipotency with atropine, systemic N-methylscopolamine should be able to block peripheral muscarinic receptors at a dose of only 0.02-0.04 mg/kg. If its target was peripheral receptors, a systemic dose of 1 mg/kg should not be necessary. When delivered directly into the lateral ventricle, a 3000 fold lower dose of only 0.3 μg/kg was sufficient to protect from seizure-induced death, supporting the hypothesis that the pharmacological target is in the brain.

These results indicate that atropine analogues have effects in the central nervous system that prevent seizure-induced apnea. High dose systemic atropine did not reduce the duration or severity of heat-induced seizures as determined by analysis of the EEG, or decrease the likelihood of Racine scale 5 seizures, but did decrease the likelihood of tonic hindlimb extension,

suggesting there were effects on forebrain seizure activity. It is not known whether an effect on seizures in the forebrain protected against apnea, or if protection was due to inhibition of forebrain projections to the brainstem or to an effect on the respiratory network. Muscarinic receptors in the medulla play an important role in respiratory control (51, 52) and central respiratory CO_2 chemoreception (53, 54). Depending on the site of action, muscarinic receptor activation can either stimulate or inhibit breathing (51, 52, 54, 69, 70). Acetylcholinesterase inhibitors block central respiratory rhythm generation via an effect in the brainstem (69, 71), and this central apnea can be prevented by atropine (72). It is possible that similar muscarinic mechanisms contribute to peri-ictal apnea in *Scn1a*$^{R1407X/+}$ mice. It is also possible that muscarinic receptors in the forebrain alter seizures (55) so they are less likely to cause apnea. Defining the specific mechanisms of apnea that are blocked by atropine analogues may help to identify methods for prevention of SUDEP.

There are many open questions about the mechanisms of death in DS mice. For example, it is not clear whether *Scn1a* mutations increase the likelihood of invasion of the brainstem by seizures, or make the respiratory network more likely to fail in response to descending input. It is not known which neurons in the brainstem express *Scn1a*, and if those neurons are involved in breathing. Seizures and death can be prevented in heterozygous *Scn1a* knockout mice with GS967, a drug that inhibits persistent sodium current (73), but it is not clear whether persistent sodium current plays a role in peri-ictal apnea.

The relationship between BSD (24), PGES (25), and peri-ictal apnea remains unclear. It is not known whether BSD occurs in our model. PGES always occurred in *Scn1a*$^{R1407X/+}$ mice that died, as was previously reported in *Lmx1b*$^{f/f/p}$ mice after MES seizures (19). BSD, PGES and apnea could all be reflective of some underlying causative mechanism, one may cause the other two, or they could be independent processes. It does not appear that PGES caused apnea since apnea often occurred before PGES (Figure 4), and because generation of the automatic respiratory rhythm in the brainstem does not require descending input from the forebrain. Further work is required to define the sequence of these and other ictal and postictal events. What is clear is that when seizures are fatal the apnea is immediate and severe. There is even complete suppression of gasping, or “autoresuscitation,” which usually occurs as a terminal event and is induced by severe hypoxia, indicating that there is such profound inhibition of the brainstem respiratory network that gasping does not even occur.

We observed that *Scn1a*$^{R1407X/+}$ mice had greater HRV than WT mice, whereas Kalume et al (40) observed that *Scn1a* knockout mice had less HRV than WT mice. This difference is likely to be methodological, as our measurements of HRV were designed for a different purpose than those of Kalume et al (40). In our study we examined the RR interval over a short time period (30-40 s) when mice were lying in their cage motionless but awake, whereas Kalume et al (40) examined the RR interval over a long period (8 hours) during a variety of normal behaviors and activity levels. There are differences in HRV under different levels of animal activity (63). We chose to use the former method as our goal was to verify block of peripheral muscarinic receptors. Kalume et al (40) measured HRV over a longer period to test the hypothesis that decreased HRV is a risk factor for SUDEP. The existing evidence does not yet support the latter hypothesis (74), although a decrease in HRV has been linked to a high risk of sudden cardiac death in humans (75). There is no evidence that the increase in HRV for short periods reported here in DS mice confers a higher risk of SUDEP, nor was that the purpose of these measurements.

It is not known how commonly death in other mouse models of SUDEP is due to the mechanisms described here. Similarly, it is not known whether the mechanisms of SUDEP in DS patients are shared with those in other types of epilepsy. However, the results presented here may also be relevant to SUDEP in other types of epilepsy, since peri-ictal apnea has previously been reported as the cause of death in $Lmx1b^{f/f/p}$, DBA and $5\text{-}HT_{2c}$ knockout mice (19, 21, 78). These differences suggest that MES-induced seizures in $Scn1a^{R1407X/+}$ mice are different than seizures that occur spontaneously or are induced by hyperthermia, and a possible clue to the mechanisms. For a seizure to induce apnea, forebrain activity must propagate to the lower brainstem where breathing is controlled. The likelihood for this may vary depending on the type of seizure, whether the relevant descending projections are engaged, and how sensitive the respiratory network is to descending input.

Cardiac abnormalities clearly play an important role in many cases of SUDEP, likely including some cases of DS, but it can be misleading to focus attention on cardiac changes without simultaneously evaluating breathing and blood gases, since changes in O_2, CO_2 and pH can induce a variety of cardiovascular abnormalities including bradycardia and tachyarrhythmias. This is of practical clinical importance, since a cardiac pacemaker would not be appropriate for preventing SUDEP in a patient with bradycardia secondary to central apnea. Instead, interventions that restore ventilation would be more logical for rescuing epilepsy patients who have peri-ictal respiratory arrest. For epilepsy patients at high risk of apnea, it would be prudent to avoid alcohol and medications that depress breathing. Stimulating arousal to re-initiate breathing or use of ventilatory assistance with a bag valve mask or mouth-to-mouth resuscitation may be more effective interventions as they would reverse a primary defect of hypoventilation.

Methods

Monitoring of DS patients with video EEG telemetry. Patients were admitted to the Pediatric EMU at Lurie Children's Hospital in Chicago, IL for routine video-EEG monitoring of refractory seizures. Seven patients with DS and convulsive seizures were selected for video analysis along with seven patients with convulsive seizures from localization-related epilepsy. Respiratory movements were difficult to visualize in some video recordings. Therefore, visualization of movements was enhanced using phase-based Eulerian video magnification motion processing (44) with MATLAB open-source software (http://people.csail.mit.edu/mrub/vidmag/). Video motion magnification processing was performed on video recordings with amplification of 4X or 10X, applying a bandpass filter of 0.05-3Hz.

To better visualize breathing in video images, a vertical line was drawn through a part of the body that showed large movements (e.g. the umbilicus in Figure 1A; Supplemental Figure 1A). Using a custom-written MATLAB script, the color value was determined at each point along the vertical line for each video frame. These values were used to create a graph with time (T; consecutive video frames) represented on the x-axis, vertical location on the y-axis (Y) and color in relative units on the z-axis (Supplemental Figure 1B). The breathing trace in this spatiotemporal YT slice was rendered more apparent by converting the image to grayscale and enhancing the contrast. The most visible single breathing trace was selected by cropping the spatiotemporal YT image (e.g. Supplemental Figure 1C-D) and drawing a line along the center of the trace (Supplemental Figure 1E) using image editing software (Corel PhotoPaint).

In a single patient (Figure 2) measurements of breathing were made using respiratory impedance plethysmography (RIP; Piezo Crystal Respiration Effort Sensors, SleepSense, Elgin, IL), $tcCO_2$ and SaO_2 (Sentec Digital Monitoring System, generously provided by SenTec AG, Therwil, Switzerland), EKG and EEG.

Mouse husbandry and genotyping.

A pair of *Scn1a*$^{R1407X/+}$ heterozygous male mice on a C3HFeB/HeJ background were generously provided by Dr. Miriam Meisler (University of Michigan, Ann Arbor, MI), and were bred with C3HFeB/HeJ female mice (Jackson Laboratory, Bar Harbor, ME) to establish a breeding colony. Breeding and genotyping of these mice have been previously described (7). Briefly, DS mice were genotyped by PCR amplification with the primers DS-F (5' CAATGATTCCTAGGGGGATGTC 3') and DS-R (5'GTTCTGTGCACTTATCTGGATTCAC 3'). Digestion of the PCR product with HpaII generated 2 fragments, 295 and 223 bp, from the wildtype allele and an uncut 518 bp fragment from the mutant allele. Genomic DNA was PCR amplified, digested with HpaII, and separated on 2% agarose gels containing 0.15 μg/ml ethidium bromide.

EEG/EMG/EKG headmount and activity/temperature telemetry implants.
EEG/EMG/EKG custom headmounts (8400-K1; Pinnacle Technology Inc.; Lawrence, KS) were implanted in P16-P22 DS mice as previously described (79). Briefly, mice received preoperative analgesia (meloxicam, 0.5 mg/kg, i.p.; or buprenorphine, 0.1 mg/kg, i.p.). Anesthesia was induced and maintained with 0.5 - 3% inhaled isoflurane. A midline skin incision was made over the skull, four holes were drilled into the skull, and a headmount was attached with two 0.1 inch (anterior) and two 0.125 inch (posterior) stainless steel machine screws (0.8*4.2; stainless steel nose pad screw; QTE North America Inc.). EMG leads extending from the posterior portion of the headmount were sutured into nuchal muscles bilaterally 3 mm from midline. EKG leads were tunneled under the skin and sutured to the anterior thoracic wall in an approximate Lead II configuration. The base of the headmount, screw heads and EMG and EKG leads were anchored with dental acrylic (Jet Acrylic; Lang Dental, Wheeling, IL) and the skin was sutured closed leaving only the headmount socket exposed. Temperature/activity telemetry probes (G2 E-Mitter; Mini-Mitter, Inc.; Bend, OR) were inserted into the peritoneal cavity to measure body temperature as previously described (79). A sterile surgical prep was made on the abdomen, and temperature probes were inserted into the peritoneum through a midline incision. The incision was closed with suture or vet-bond (3M Animal Care Product, St. Paul, MN). Animals received post-operative analgesia with meloxicam (0.5 mg/kg, i.p.) or buprenorphine (0.1 mg/kg, i.p.) for 3 days, and were allowed to recover for at least 5 days before recordings were made.

Long-term (24/7) continuous mouse EMU /plethysmography data acquisition. A preamplifier (8406-SE31M-C Pinnacle Technology Inc.; Lawrence, KS) was inserted into the implanted headmount connector for recording EEG, EKG and EMG (gain 10x; high pass filter for EKG 0.5 Hz; EEG 1 Hz; EMG 10 Hz). The animal was placed into a mouse EMU / plethysmography chamber custom-designed and built to comply with requirements for continuous housing described in the Guide for the Care and Use of Laboratory Animals, 8th edition (80). The floor was circular and 5 inches in diameter. The walls were semiconical with a roof that was 5.5 inches high and 3 inches in diameter. The chamber volume was 815 ml. There were ports for air in and air out, and for pressure and temperature/humidity monitoring. The chamber was supplied with continuous flow of room air at ~400 ml/min via supply and exhaust air pumps (MK-1504 Aquarium Air Pump; AQUA Culture, Bentonville, AR) balanced

to maintain chamber pressure near atmospheric. Mice had access to a continuous supply of water and food.

The EMU / plethysmography chamber pressure was measured using a digital differential pressure transducer (SDP610-25Pa; Sensirion AG, Switzerland). Chamber temperature and relative humidity were also continuously monitored (HIH-6130 sensor; Honeywell International Inc., Golden Valley, MN). Signal outputs from the pressure transducer and temperature/humidity sensor were connected to a microcontroller (Teensy 3.1; PJRC.com, Sherwood, OR) using a custom-designed printed circuit board. The digital transducers and microcontroller communicated through an I^2C interface via the Arduino platform (ARDUINO 1.6.9; Arduino.cc, and Teensyduino 1.28; PJRC.com, Sherwood, OR) to upload configuration code of the digital sensors to the microcontroller board. Chamber temperature, relative humidity and pressure were acquired continuously at 100 Hz through a USB port with data acquisition software custom-written in MATLAB (Mathworks Co.; Natick, MA). Breathing caused changes in pressure in the chamber due to heating and humidification of inspired air based on well-established physical principles, and these were used to calculate changes in lung volume (81).

EEG, EMG and EKG leads were tethered to a commutator (#8408; Pinnacle Technology Inc; Lawrence, KS) and connected to an amplifier (Model 440 Instrumentation Amplifier; Brownlee Precision Co.; San Jose, CA) where signals were amplified by 10x and band-pass filtered (EEG - 0.3 to 400 Hz; EMG - 10 to 500 Hz; EKG - 1 to 500 Hz). These signals were digitized with an analog-to-digital converter (PCI-6225, National Instruments Corp., Austin, TX) in a desktop computer and acquired with the same custom-written MATLAB data acquisition software. Body temperature and activity were captured by a telemetry receiver (ER-4000, Energizer Receiver; Mini-Mitter, Inc., Bend, OR) placed beneath the recording chamber, transmitted to the computer via a serial port, and sampled every 10 seconds with the same custom-written MATLAB data acquisition software. All digitized data were saved on external hard drives.

Monitoring of spontaneous deaths in mice. One cohort of *Scn1a*$^{R1407X/+}$ mice (n=78) were monitored for spontaneous deaths using video recording only (Figure 3). Uninstrumented mice were housed in their home cages and continuous video monitoring was performed from the age of P16 to P60. Video recordings were made at 30 frames per second using a night-vision web camera (FL8910W; Foscam Digital Technologies, Houston, TX). Up to 32 cameras were connected to a single computer and video recordings were stored on an external hard drive using commercial video webcam software (Blue Iris 4; Foscam Digital Technologies, Houston, TX). When a mouse was found dead in a cage, the video was reviewed to determine the time of death and whether death was preceded by a behavioral seizure.

A second cohort of *Scn1a*$^{R1407X/+}$ mice (n=19) were monitored for spontaneous deaths over 195 days using video recording as well as EEG, EMG, EKG, breathing, temperature and activity. Each recording session lasted up to 24 hours, after which the EMU was opened and cleaned. Mice were then returned to the EMU for continued monitoring or to their home cage. While in the EMU, mice had free access to food and water. Long-term mouse EMU data were continuously stored on an external hard drive (DRDR5A21-20TB, DroboWorks.com, Irvine, CA). From 4,223 total hours of recording from 19 mice between P23-P40, two mice died spontaneously. When these mice died, monitoring was terminated and data were reviewed to assess the cause of death.

Heat-induced seizures in mice. Mice were instrumented with headmounts and telemetry probes to allow recordings of all the signals described for monitoring spontaneous deaths. After at least five days mice were lightly anesthetized with 1% isoflurane for 1-2 minutes to connect a preamplifier to the headmount. Any experimental drugs were injected at that time. Mice were then placed in the plethysmography chamber and allowed to recover from anesthesia and acclimate for 30 minutes. Seizures were then induced by hyperthermia using a protocol previously reported for a Dravet Syndrome mouse model (40). Using a heat lamp, body temperature in *Scn1a*$^{R1407X/+}$ mice and WT littermates was increased from 36 to 42.5 °C at a rate of 0.5 °C per minute, or until a generalized seizure with tonic hindlimb extension was induced. To maximize the amplitude of the breathing signal, the plethysmography chamber was maintained at 25-27 °C by a Peltier device that cooled the incoming air. In some cases mice were resuscitated after a seizure by placing Tygon tubing over the snout and inflating the lungs with air using a mechanical ventilator (MiniVent type 845; Harvard Apparatus, Holliston, MA).

Effect of muscarinic receptor antagonists on bradycardia. To determine the role of parasympathetic output in postictal bradycardia, muscarinic receptor antagonists were administered 30 minutes prior to heat-induced seizures. All antagonists given via intraperitoneal injection were dissolved in a volume of 50 µl in bacteriostatic 0.9% NaCl solution. In a separate set of experiments, N-methylscopolamine was given via injection into the lateral ventricle dissolved to a volume of 50 nl in artificial cerebrospinal fluid (aCSF) containing (in mM): 125 NaCl, 5.0 KCl, 24 $NaHCO_3$, 1.25 KH_2PO_4, 0.8 $CaCl_2$, 1.25 $MgSO_4$, 30 glucose. Coordinates used for i.c.v. injection were 0 mm AP to Bregma, 1.0 mm lateral, and 2.5 mm below the skull surface. Atropine, methylatropine nitrate, and N-methylscopolamine bromide were obtained from Sigma Aldrich. At a dose of 1 mg/kg (i.p.), atropine had no effect on the likelihood of Racine scale 5 seizures, or the duration or severity of seizures based on EEG analysis. In the cohort of control mice shown in Figure 5A for fatal seizures (n=7), seizure duration was 25.7±9.2 seconds and the mean EEG power between 0.5 and 20 Hz (as a measure of seizure severity) was 0.083±0.026 s^{-1}. In contrast, for the mice treated with atropine shown in Figure 5A for non-fatal seizures (n=14 seizures), seizure duration was 21.9±8.3 seconds and the mean EEG power was 0.121±0.055 s^{-1}. These differences were not statistically significant ($p>0.05$; Mann-Whitney U test). After treatment with atropine (1 mg/kg ip) or N-methylscopolamine (0.3 µg/kg i.c.v.) some seizures were characterized by clonic limb contractions instead of tonic hindlimb extension, although in both cases they met criteria for Racine scale 5 seizures.

HRV was assessed using Poincaré plots (65) before and 30 minutes after administering muscarinic receptor antagonists. This method graphs the time between one pair of QRS complexes on an EKG (R-R' interval) versus the time between the next pair of QRS complexes (R'-R"). The standard deviation of the points along the unity line is termed long term adaptation (SD2), and the standard deviation of the points perpendicular to the unity line is referred to as short term adaptation (SD1). HRV is primarily due to vagus nerve mediated parasympathetic inhibition of the sinoatrial node (60-65). For all Poincaré plots, 500 pairs of RR intervals were plotted and analyzed at baseline and after drug injection. Data were not analyzed during any animal movements to eliminate artifacts.

Exposure to hypoxia. *Scn1a*$^{R1407X/+}$ mice and WT littermates were instrumented with EKG leads and temperature probes as above. After at least 5 days of recovery, mice were placed in a plethysmography chamber where the EKG and body temperature were continuously monitored. The chamber was flushed with gas flowing at 700 ml/min, first with medical grade 21% O_2 /

79% N_2 / 1% isoflurane. After establishing a baseline, the gas was switched to 100% N_2 / 1% isoflurane. Isoflurane levels were maintained at 1% using a precision vaporizer (Summit Anesthesia Solutions, Bend, Oregon). The time course for the change of PO_2 was measured using an O_2 analyzer (Model S-3A, AEI Technologies, Pittsburgh, PA) in a separate set of experiments without isoflurane to avoid damage to the O_2 analyzer. Mice were studied either with or without injection of atropine (1 mg/kg, i.p.) 30 min before exposure to anoxia. Control mice were injected with the same volume of saline solution. The plethysmograph chamber was maintained at 30 °C using a heat lamp and feedback controller (TCAT-2AC; Physitemp Instr., Clifton, New Jersey).

Data analysis and statistics. Time-frequency power spectrum analysis was performed with MATLAB based on a short-time Fast Fourier Transform (FFT). The time-dependent power spectrum density of the signal was computed and displayed with discrete-time epochs calculated for 0.5 second intervals. Sections overlapped by 20% to smooth the signal. The EKG sampling rate was 1 kHz, while EEG, EMG, and plethysmography were sampled at 100 Hz.

Analyses of respiratory rate and heart rate were performed using software custom-written in MATLAB and/or Clampfit Software (Molecular Devices, Sunnyvale, CA). Inspiratory peaks were detected automatically from plethysmography data by applying a bandpass filter of 1 – 10 Hz and using peak detection verified manually. R-wave detection of EKG data was performed by applying a continuous wavelet transform and peak detection in MATLAB. The time interval between breath peaks (interbreath interval; IBI) and the R-R interval from detected R-waves were computed as the mean for 10s epochs.

Abnormal breathing in DS patients was compared to localization-related epilepsy patients (Table 1) using a Chi square test. Severity of seizures was measured by computing the mean EEG intensity from power spectra generated using MATLAB. Statistical comparisons of seizure severity and duration, and Poincarè plots (SD-1 and SD-2) were made using a Mann-Whitney U Test with an overall significance level set to $p<0.05$ (GraphPad Prism V6.01). When data is presented as X ± Y, X is the group mean and Y is the standard deviation. All error bars on graphs represent the standard error of the mean.

Clinical phenotype of DS patient with prolonged postictal hypoventilation. The patient shown in Figure 2 had her first seizure at 5.5 months of age. Seizure types prior to the EMU admission had included generalized convulsions, hemiconvulsions, partial seizures with variable semiology, atypical absence seizures, and myoclonic jerks. At the time of EMU admission, seizure types included: 1) Feeling “spacey” for 5-10 seconds with blank staring, slackening of facial muscles, and slurred speech, and; 2) Repetitive asynchronous generalized convulsions in series lasting 1-2 minutes each, interrupted by a fixed gaze for up to five minutes. The patient’s seizures had worsened in frequency and severity during the previous six months. There was concern for a decrease in alertness and cognitive ability. The EMU study was performed to assess EEG background activity and to clarify the types of seizures. She was treated at the time of admission with levetiracetam, clobazam, stiripentol and a ketogenic diet. The first event for the episode shown in Figure 2 began off camera in the bathroom after the mother reported that the patient had an increase in “staring” episodes. During the seizures the EEG showed generalized onset of high amplitude, diffuse, spike/polyspike wave discharges that evolved in amplitude and frequency. These ictal abnormalities terminated abruptly with generalized slowing. Interictal discharges would quickly reappear, and coalesce just prior to the next convulsive seizure.

Study approval

Human studies: All experimental protocols were approved by the Northwestern University Institutional Review Board and performed under the direct supervision of a faculty neurologist. Written informed consent from participants or their guardians was obtained.

Animal studies: All procedures and experiments involving mice were carried out with approval of the University of Iowa Institutional Animal Care and Use Committee, and in strict accordance with the recommendations of the Guide for the Care and Use of Laboratory Animals, 8th edition (80). The minimum possible number of animals was used, and care was taken to reduce any discomfort.

Author contributions

YK designed and built the experimental apparatus used for mouse experiments, carried out the spontaneous death and mouse survival experiments, wrote data acquisition and analysis software, analyzed data, instantiated the Eulerian Video magnification of videos, and wrote the manuscript. EB designed and carried out the mouse experiments on hyperthermia induced seizures, peripheral parasympathetic blockade, i.c.v. injection of N-methylscopolamine and hypoxia, analyzed that data, and edited the manuscript. CKT & LAS carried out the mouse survival experiments, and edited the manuscript. BKG contributed to the design, analysis and interpretation of cardiorespiratory data from humans and mice, and edited the manuscript. SHK, DRN, and LL collected data from the Dravet syndrome patients, analyzed that data and edited the manuscript. GBR oversaw the work, helped design all experiments, analyzed data, and edited the manuscript.

Acknowledgements

NIH U01 NS 090414 (YK, EB, CKT, LAS, BKG & GBR), and the Beth L. Tross Epilepsy Research Fund (GBR).

References

1. Devinsky O, Hesdorffer DC, Thurman DJ, Lhatoo S, and Richerson G. Sudden unexpected death in epilepsy: epidemiology, mechanisms, and prevention. *Lancet neurology.* 2016;15(10):1075-88.
2. Ryvlin P, Nashef L, Lhatoo SD, Bateman LM, Bird J, Bleasel A, Boon P, Crespel A, Dworetzky BA, Hogenhaven H, et al. Incidence and mechanisms of cardiorespiratory arrests in epilepsy monitoring units (MORTEMUS): a retrospective study. *Lancet neurology.* 2013;12(10):966-77.
3. Langan Y, Nashef L, and Sander JW. Sudden unexpected death in epilepsy: a series of witnessed deaths. *Journal of neurology, neurosurgery, and psychiatry.* 2000;68(2):211-3.
4. Surges R, Thijs RD, Tan HL, and Sander JW. Sudden unexpected death in epilepsy: risk factors and potential pathomechanisms. *Nature reviews Neurology.* 2009;5(9):492-504.
5. Massey CA, Sowers LP, Dlouhy BJ, and Richerson GB. Mechanisms of sudden unexpected death in epilepsy: the pathway to prevention. *Nature reviews Neurology.* 2014;10(5):271-82.
6. Moseley B, Bateman L, Millichap JJ, Wirrell E, and Panayiotopoulos CP. Autonomic epileptic seizures, autonomic effects of seizures, and SUDEP. *Epilepsy & behavior : E&B.* 2013;26(3):375-85.
7. Auerbach DS, Jones J, Clawson BC, Offord J, Lenk GM, Ogiwara I, Yamakawa K, Meisler MH, Parent JM, and Isom LL. Altered cardiac electrophysiology and SUDEP in a model of Dravet syndrome. *PloS one.* 2013;8(10):e77843.
8. van der Lende M, Surges R, Sander JW, and Thijs RD. Cardiac arrhythmias during or after epileptic seizures. *Journal of neurology, neurosurgery, and psychiatry.* 2016;87(1):69-74.
9. Surges R, Adjei P, Kallis C, Erhuero J, Scott CA, Bell GS, Sander JW, and Walker MC. Pathologic cardiac repolarization in pharmacoresistant epilepsy and its potential role in sudden unexpected death in epilepsy: a case-control study. *Epilepsia.* 2010;51(2):233-42.
10. Johnson JN, Hofman N, Haglund CM, Cascino GD, Wilde AA, and Ackerman MJ. Identification of a possible pathogenic link between congenital long QT syndrome and epilepsy. *Neurology.* 2009;72(3):224-31.
11. Glasscock E, Yoo JW, Chen TT, Klassen TL, and Noebels JL. Kv1.1 potassium channel deficiency reveals brain-driven cardiac dysfunction as a candidate mechanism for sudden unexplained death in epilepsy. *The Journal of neuroscience.* 2010;30(15):5167-75.
12. Delogu AB, Spinelli A, Battaglia D, Dravet C, De Nisco A, Saracino A, Romagnoli C, Lanza GA, and Crea F. Electrical and autonomic cardiac function in patients with Dravet syndrome. *Epilepsia.* 2011;52 Suppl 2(55-8.
13. DeGiorgio CM, Miller P, Meymandi S, Chin A, Epps J, Gordon S, Gornbein J, and Harper RM. RMSSD, a measure of vagus-mediated heart rate variability, is associated with risk factors for SUDEP: the SUDEP-7 Inventory. *Epilepsy & behavior : E&B.* 2010;19(1):78-81.
14. Moseley BD, Wirrell EC, Nickels K, Johnson JN, Ackerman MJ, and Britton J. Electrocardiographic and oximetric changes during partial complex and generalized seizures. *Epilepsy research.* 2011;95(3):237-45.
15. Surges R, Henneberger C, Adjei P, Scott CA, Sander JW, and Walker MC. Do alterations in inter-ictal heart rate variability predict sudden unexpected death in epilepsy? *Epilepsy research.* 2009;87(2-3):277-80.

16. Nashef L, Walker F, Allen P, Sander JW, Shorvon SD, and Fish DR. Apnoea and bradycardia during epileptic seizures: relation to sudden death in epilepsy. *Journal of neurology, neurosurgery, and psychiatry.* 1996;60(3):297-300.
17. Bateman LM, Li CS, and Seyal M. Ictal hypoxemia in localization-related epilepsy: analysis of incidence, severity and risk factors. *Brain : a journal of neurology.* 2008;131(Pt 12):3239-45.
18. Zhan Q, Buchanan GF, Motelow JE, Andrews J, Vitkovskiy P, Chen WC, Serout F, Gummadavelli A, Kundishora A, Furman M, et al. Impaired Serotonergic Brainstem Function during and after Seizures. *The Journal of neuroscience.* 2016;36(9):2711-22.
19. Buchanan GF, Murray NM, Hajek MA, and Richerson GB. Serotonin neurones have anti-convulsant effects and reduce seizure-induced mortality. *The Journal of physiology.* 2014;592(Pt 19):4395-410.
20. Dlouhy BJ, Gehlbach BK, Kreple CJ, Kawasaki H, Oya H, Buzza C, Granner MA, Welsh MJ, Howard MA, Wemmie JA, et al. Breathing Inhibited When Seizures Spread to the Amygdala and upon Amygdala Stimulation. *The Journal of neuroscience.* 2015;35(28):10281-9.
21. Feng HJ, and Faingold CL. Abnormalities of serotonergic neurotransmission in animal models of SUDEP. *Epilepsy & behavior : E&B.* 2015.
22. Nakase K, Kollmar R, Lazar J, Arjomandi H, Sundaram K, Silverman J, Orman R, Weedon J, Stefanov D, Savoca E, et al. Laryngospasm, central and obstructive apnea during seizures: Defining pathophysiology for sudden death in a rat model. *Epilepsy research.* 2016;128(126-39.
23. Seyal M, Bateman LM, Albertson TE, Lin TC, and Li CS. Respiratory changes with seizures in localization-related epilepsy: analysis of periictal hypercapnia and airflow patterns. *Epilepsia.* 2010;51(8):1359-64.
24. Aiba I, and Noebels JL. Spreading depolarization in the brainstem mediates sudden cardiorespiratory arrest in mouse SUDEP models. *Science translational medicine.* 2015;7(282):282ra46.
25. Lhatoo SD, Faulkner HJ, Dembny K, Trippick K, Johnson C, and Bird JM. An electroclinical case-control study of sudden unexpected death in epilepsy. *Annals of neurology.* 2010;68(6):787-96.
26. Goldman AM. Genetics of SUDEP: an overview. *Epilepsia.* 2015.
27. Aurlien D, Leren TP, Tauboll E, and Gjerstad L. New SCN5A mutation in a SUDEP victim with idiopathic epilepsy. *Seizure : the journal of the British Epilepsy Association.* 2009;18(2):158-60.
28. Hata Y, Yoshida K, Kinoshita K, and Nishida N. Epilepsy-Related Sudden Unexpected Death: Targeted Molecular Analysis of Inherited Heart Disease Genes using Next-Generation DNA Sequencing. *Brain Pathol.* 2016.
29. Parisi P, Oliva A, Coll Vidal M, Partemi S, Campuzano O, Iglesias A, Pisani D, Pascali VL, Paolino MC, Villa MP, et al. Coexistence of epilepsy and Brugada syndrome in a family with SCN5A mutation. *Epilepsy research.* 2013;105(3):415-8.
30. Tiron C, Campuzano O, Perez-Serra A, Mademont I, Coll M, Allegue C, Iglesias A, Partemi S, Striano P, Oliva A, et al. Further evidence of the association between LQT syndrome and epilepsy in a family with KCNQ1 pathogenic variant. *Seizure : the journal of the British Epilepsy Association.* 2015;25(65-7.
31. Dravet C. The core Dravet syndrome phenotype. *Epilepsia.* 2011;52 Suppl 2(3-9.

32. Parihar R, and Ganesh S. The SCN1A gene variants and epileptic encephalopathies. *J Hum Genet.* 2013;58(9):573-80.
33. Hani AJ, Mikati HM, and Mikati MA. Genetics of pediatric epilepsy. *Pediatr Clin North Am.* 2015;62(3):703-22.
34. Claes L, Del-Favero J, Ceulemans B, Lagae L, Van Broeckhoven C, and De Jonghe P. De novo mutations in the sodium-channel gene SCN1A cause severe myoclonic epilepsy of infancy. *American journal of human genetics.* 2001;68(6):1327-32.
35. Sakauchi M, Oguni H, Kato I, Osawa M, Hirose S, Kaneko S, Takahashi Y, Takayama R, and Fujiwara T. Retrospective multiinstitutional study of the prevalence of early death in Dravet syndrome. *Epilepsia.* 2011;52(6):1144-9.
36. Cooper MS, McIntosh A, Crompton DE, McMahon JM, Schneider A, Farrell K, Ganesan V, Gill D, Kivity S, Lerman-Sagie T, et al. Mortality in Dravet syndrome. *Epilepsy research.* 2016;128(43-7.
37. Ergul Y, Ekici B, Tatli B, Nisli K, and Ozmen M. QT and P wave dispersion and heart rate variability in patients with Dravet syndrome. *Acta Neurol Belg.* 2013;113(2):161-6.
38. Daverio M, Ciccone O, Boniver C, De Palma L, Corrado D, and Vecchi M. Supraventricular Tachycardia During Status Epilepticus in Dravet Syndrome: A Link Between Brain and Heart? *Pediatr Neurol.* 2016;56(69-71.
39. Ogiwara I, Miyamoto H, Morita N, Atapour N, Mazaki E, Inoue I, Takeuchi T, Itohara S, Yanagawa Y, Obata K, et al. Nav1.1 localizes to axons of parvalbumin-positive inhibitory interneurons: a circuit basis for epileptic seizures in mice carrying an Scn1a gene mutation. *The Journal of neuroscience.* 2007;27(22):5903-14.
40. Kalume F, Westenbroek RE, Cheah CS, Yu FH, Oakley JC, Scheuer T, and Catterall WA. Sudden unexpected death in a mouse model of Dravet syndrome. *The Journal of clinical investigation.* 2013;123(4):1798-808.
41. Maier SK, Westenbroek RE, Yamanushi TT, Dobrzynski H, Boyett MR, Catterall WA, and Scheuer T. An unexpected requirement for brain-type sodium channels for control of heart rate in the mouse sinoatrial node. *Proceedings of the National Academy of Sciences of the United States of America.* 2003;100(6):3507-12.
42. Maier SK, Westenbroek RE, Schenkman KA, Feigl EO, Scheuer T, and Catterall WA. An unexpected role for brain-type sodium channels in coupling of cell surface depolarization to contraction in the heart. *Proceedings of the National Academy of Sciences of the United States of America.* 2002;99(6):4073-8.
43. Cheah CS, Yu FH, Westenbroek RE, Kalume FK, Oakley JC, Potter GB, Rubenstein JL, and Catterall WA. Specific deletion of NaV1.1 sodium channels in inhibitory interneurons causes seizures and premature death in a mouse model of Dravet syndrome. *Proceedings of the National Academy of Sciences of the United States of America.* 2012;109(36):14646-51.
44. Wu HY, Rubinstein M, Shih E, Guttag J, Durand F, and Freeman WT. Eulerian Video Magnification for Revealing Subtle Changes in the World. *ACM Transactions on Graphics.* 2012;31(4).
45. Cao D, Ohtani H, Ogiwara I, Ohtani S, Takahashi Y, Yamakawa K, and Inoue Y. Efficacy of stiripentol in hyperthermia-induced seizures in a mouse model of Dravet syndrome. *Epilepsia.* 2012;53(7):1140-5.

46. Gargiulo S, Greco A, Gramanzini M, Esposito S, Affuso A, Brunetti A, and Vesce G. Mice anesthesia, analgesia, and care, Part I: anesthetic considerations in preclinical research. *ILAR J.* 2012;53(1):E55-69.
47. Flecknell PA. Anaesthesia of animals for biomedical research. *British journal of anaesthesia.* 1993;71(6):885-94.
48. Hawk CT, Leary SL, and Morris TH. *Formulary for Laboratory Animals. Third Edition.* Ames, IA: Blackwell Publishing; 2005.
49. Proakis AG, and Harris GB. Comparative penetration of glycopyrrolate and atropine across the blood--brain and placental barriers in anesthetized dogs. *Anesthesiology.* 1978;48(5):339-44.
50. Houze P, Pronzola L, Kayouka M, Villa A, Debray M, and Baud FJ. Ventilatory effects of low-dose paraoxon result from central muscarinic effects. *Toxicology and applied pharmacology.* 2008;233(2):186-92.
51. Muere C, Neumueller S, Miller J, Olesiak S, Hodges MR, Pan L, and Forster HV. Atropine microdialysis within or near the pre-Botzinger Complex increases breathing frequency more during wakefulness than during NREM sleep. *J Appl Physiol (1985).* 2013;114(5):694-704.
52. Mallios VJ, Lydic R, and Baghdoyan HA. Muscarinic receptor subtypes are differentially distributed across brain stem respiratory nuclei. *The American journal of physiology.* 1995;268(6 Pt 1):L941-9.
53. Dev NB, and Loeschcke HH. A cholinergic mechanism involved in the respiratory chemosensitivity of the medulla oblongata in the cat. *Pflugers Archiv : European journal of physiology.* 1979;379(1):29-36.
54. Nattie EE, Wood J, Mega A, and Goritski W. Rostral ventrolateral medulla muscarinic receptor involvement in central ventilatory chemosensitivity. *J Appl Physiol (1985).* 1989;66(3):1462-70.
55. Turski L, Ikonomidou C, Turski WA, Bortolotto ZA, and Cavalheiro EA. Review: cholinergic mechanisms and epileptogenesis. The seizures induced by pilocarpine: a novel experimental model of intractable epilepsy. *Synapse.* 1989;3(2):154-71.
56. Brezenoff HE, Xiao YF, and Vargas H. A comparison of the central and peripheral antimuscarinic effects of atropine and methylatropine injected systemically and into the cerebral ventricles. *Life sciences.* 1988;42(8):905-11.
57. Herz A, Teschemacher H, Hofstetter A, and Kurz H. The Importance of Lipid-Solubility for the Central Action of Cholinolytic Drugs. *Int J Neuropharmacol.* 1965;4(207-18.
58. Witter A, Slangen JL, and Terpstra GK. Distribution of ^{3}H-methylatropine in rat brain. *Neuropharmacology.* 1973;12(9):835-41.
59. Paul-David J, Riehl JL, and Unna KR. Quantification of effects of depressant drugs on EEG activation response. *The Journal of pharmacology and experimental therapeutics.* 1960;129(69-74.
60. Taylor JA, Carr DL, Myers CW, and Eckberg DL. Mechanisms underlying very-low-frequency RR-interval oscillations in humans. *Circulation.* 1998;98(6):547-55.
61. Fouad FM, Tarazi RC, Ferrario CM, Fighaly S, and Alicandri C. Assessment of parasympathetic control of heart rate by a noninvasive method. *The American journal of physiology.* 1984;246(6 Pt 2):H838-42.
62. Thireau J, Zhang BL, Poisson D, and Babuty D. Heart rate variability in mice: a theoretical and practical guide. *Experimental physiology.* 2008;93(1):83-94.

63. Tsai ML, Chen CC, Yeh CJ, Chou LM, and Cheng CH. Frequency ranges of heart rate variability related to autonomic nerve activity in the mouse. *Clin Exp Hypertens.* 2012;34(3):182-90.
64. Gehrmann J, Hammer PE, Maguire CT, Wakimoto H, Triedman JK, and Berul CI. Phenotypic screening for heart rate variability in the mouse. *American journal of physiology Heart and circulatory physiology.* 2000;279(2):H733-40.
65. Kamen PW, Krum H, and Tonkin AM. Poincare plot of heart rate variability allows quantitative display of parasympathetic nervous activity in humans. *Clin Sci (Lond).* 1996;91(2):201-8.
66. Chen KC, and McGrath JJ. Response of the isolated heart to carbon monoxide and nitrogen anoxia. *Toxicology and applied pharmacology.* 1985;81(3 Pt 1):363-70.
67. Carreras A, Wang Y, Gozal D, Montserrat JM, Navajas D, and Farre R. Non-invasive system for applying airway obstructions to model obstructive sleep apnea in mice. *Respiratory physiology & neurobiology.* 2011;175(1):164-8.
68. Kannurpatti SS, Biswal BB, and Hudetz AG. Differential fMRI-BOLD signal response to apnea in humans and anesthetized rats. *Magn Reson Med.* 2002;47(5):864-70.
69. Gaspari RJ, and Paydarfar D. Dichlorvos-induced central apnea: effects of selective brainstem exposure in the rat. *Neurotoxicology.* 2011;32(2):206-14.
70. Lydic R, and Baghdoyan HA. Pedunculopontine stimulation alters respiration and increases ACh release in the pontine reticular formation. *The American journal of physiology.* 1993;264(3 Pt 2):R544-54.
71. Gillis RA, Walton DP, Quest JA, Namath IJ, Hamosh P, and Dretchen KL. Cardiorespiratory effects produced by activation of cholinergic muscarinic receptors on the ventral surface of the medulla. *The Journal of pharmacology and experimental therapeutics.* 1988;247(2):765-73.
72. Fleming NW, Henderson TR, and Dretchen KL. Mechanisms of respiratory failure produced by neostigmine and diisopropyl fluorophosphate. *European journal of pharmacology.* 1991;195(1):85-91.
73. Anderson LL, Hawkins NA, Thompson CH, Kearney JA, and George AL, Jr. Unexpected Efficacy of a Novel Sodium Channel Modulator in Dravet Syndrome. *Sci Rep.* 2017;7(1):1682.
74. Harden C, Tomson T, Gloss D, Buchhalter J, Cross JH, Donner E, French JA, Gil-Nagel A, Hesdorffer DC, Smithson WH, et al. Practice guideline summary: Sudden unexpected death in epilepsy incidence rates and risk factors: Report of the Guideline Development, Dissemination, and Implementation Subcommittee of the American Academy of Neurology and the American Epilepsy Society. *Neurology.* 2017;88(17):1674-80.
75. Stein PK, Domitrovich PP, Huikuri HV, Kleiger RE, and Cast I. Traditional and nonlinear heart rate variability are each independently associated with mortality after myocardial infarction. *Journal of cardiovascular electrophysiology.* 2005;16(1):13-20.
76. Thurman DJ, Hesdorffer DC, and French JA. Sudden unexpected death in epilepsy: assessing the public health burden. *Epilepsia.* 2014;55(10):1479-85.
77. Sveinsson O, Andersson T, Carlsson S, and Tomson T. The incidence of SUDEP: A nationwide population-based cohort study. *Neurology.* 2017;89(2):170-7.
78. Tecott LH, Sun LM, Akana SF, Strack AM, Lowenstein DH, Dallman MF, and Julius D. Eating disorder and epilepsy in mice lacking 5-HT2c serotonin receptors. *Nature.* 1995;374(6522):542-6.

79. Buchanan GF, and Richerson GB. Central serotonin neurons are required for arousal to CO2. *Proceedings of the National Academy of Sciences of the United States of America.* 2010;107(37):16354-9.
80. ACP. *Guide for the Care and Use of Laboratory Animals.* Washington, DC: National Academies Press; 2011.
81. Drorbaugh JE, and Fenn WO. A barometric method for measuring ventilation in newborn infants. *Pediatrics.* 1955;16(1):81-7.

Figure legends

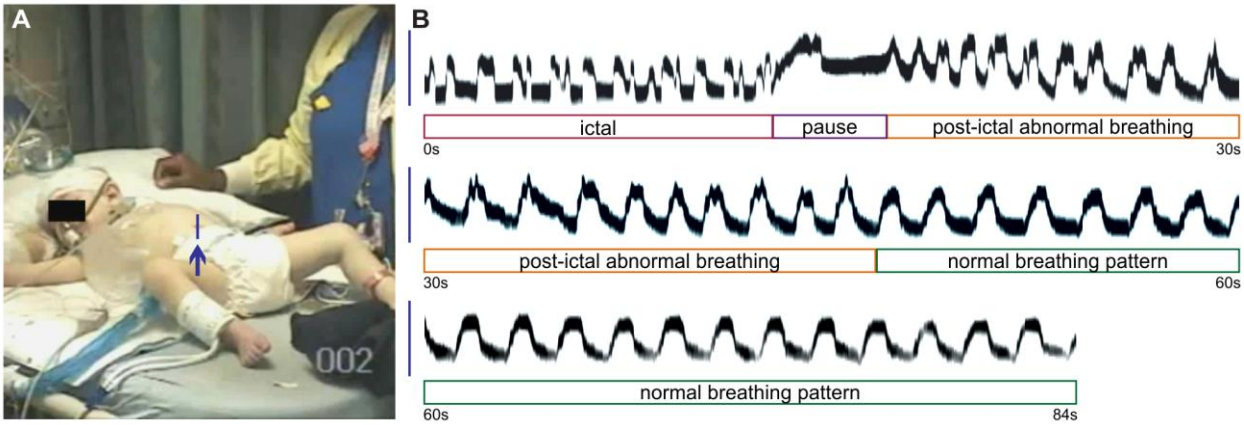

Figure 1. Seizures induce ataxic breathing in a DS patient. (A, B) Irregular breathing during and after a seizure. Video frame (A) from Supplemental Video 1 showing region of interest (vertical line pointed to by arrow) used to visualize respiratory movements. Using the methods illustrated in Supplemental Figure 1A, respiratory movements were plotted during and after a generalized seizure (B; traces are contiguous). During the seizure (1st 13 seconds) most inspirations had more than one peak. Immediately after the seizure there was a respiratory pause followed by continued abnormal inspirations lasting until 32 seconds postictal. A normal breathing pattern then resumed with regular, monophasic inspiratory efforts.

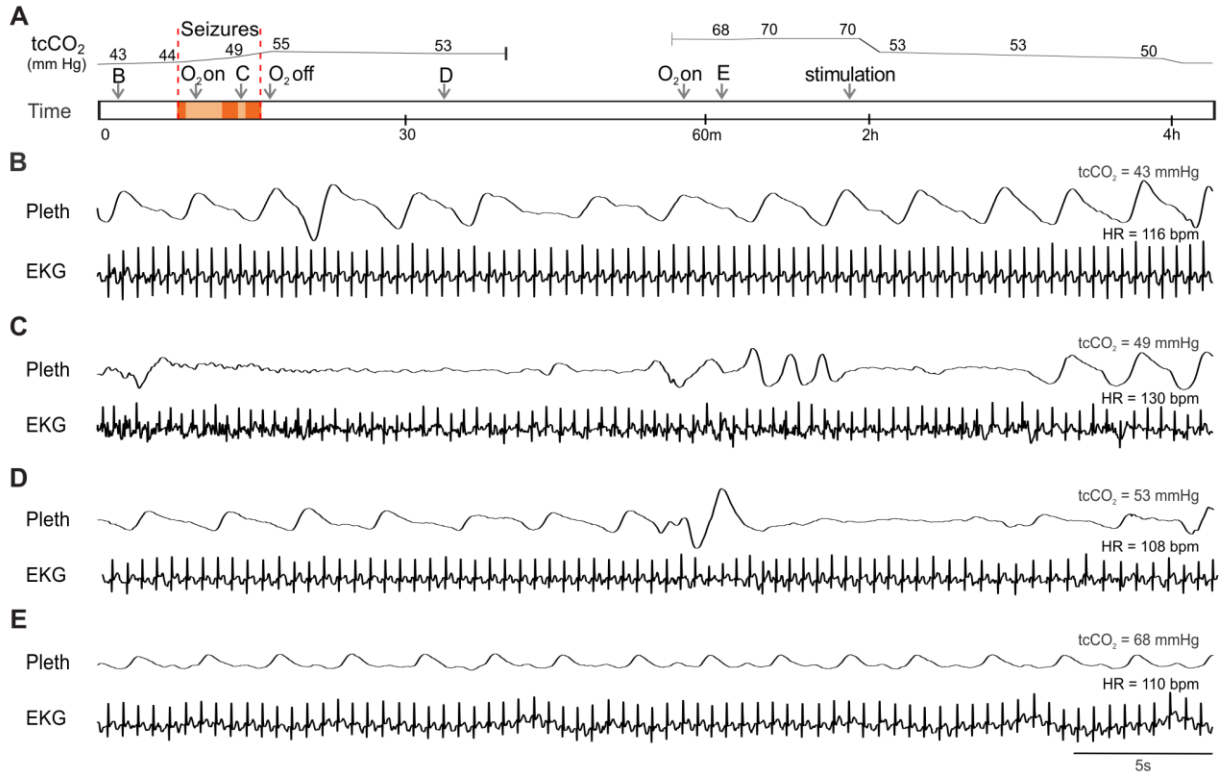

Figure 2. Prolonged postictal hypoventilation in a DS patient. (A) Schematic of events while recording cardiorespiratory activity during and after a seizure in a 9 year old girl with DS. The numbers above the upper line in A are measured values of $tcCO_2$. The upper line shows the approximate time course of the changes in $tcCO_2$. Arrows labeled "B-E" denote the time of recordings shown in parts B-E. Arrows also denote when supplemental O_2 was administered or discontinued, and when the patient was stimulated to cause arousal. Red shading denotes convulsive seizures and orange shading denotes periods of decreased responsiveness and EEG slowing. (B-E) Respiratory impedance plethysmography (Pleth) and EKG during normal breathing when $tcCO_2$ was 44 mmHg (B), between convulsive seizures (C), after the seizures when $tcCO_2$ had risen to 53 mmHg (D), and 44 minutes after the seizures when $tcCO_2$ had risen to 68 mmHg (E). At 2 hours, $tcCO_2$ decreased when the patient was stimulated to arouse, but did not return to baseline until 4 hours.

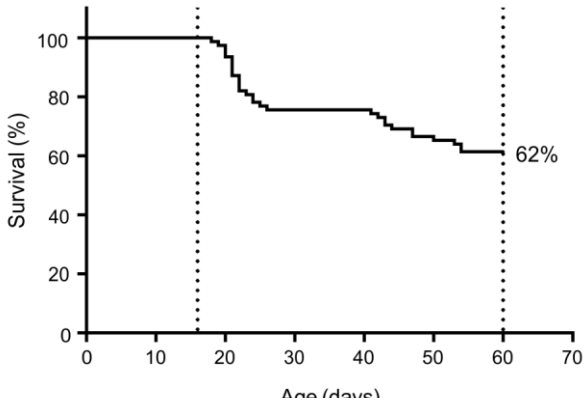

Figure 3. Survival curve of *Scn1a*$^{R1407X/+}$ mice. Video monitoring revealed that 38% (n=30 of 78) of *Scn1a*$^{R1407X/+}$ mice spontaneously died between the ages of P20 and P60. All of these spontaneous deaths occurred after Racine scale 5 generalized seizures with tonic hindlimb extension.

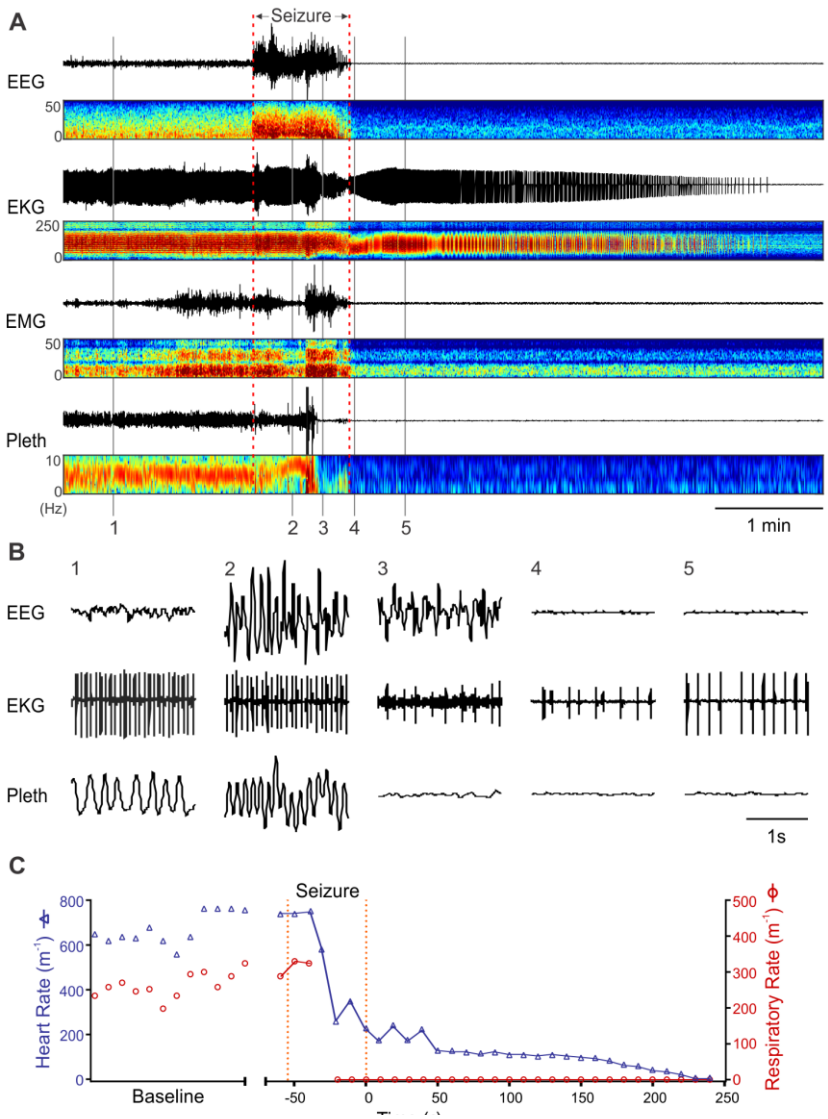

Figure 4. Death of an *Scn1a*$^{R1407X/+}$ mouse (P40) after a spontaneous seizure was due to respiratory arrest followed by secondary bradycardia. (A) Events leading to death. Traces from top down are EEG, EKG, EMG and whole animal plethysmography, in each case with paired power spectrum heat maps. A spontaneous seizure occurred at the time indicated, and this was followed by PGES in the EEG. Shortly after the onset of the seizure, breathing became disrupted. Respiratory activity ceased halfway through the seizure. In contrast, the EKG did not change until near the end of the seizure, after which the frequency and amplitude slowly decreased over the next four minutes. Note there was some movement artifact on the plethysmography trace half way through the seizure. (B) Expanded traces of EEG, EKG and plethysmography at the times labelled 1-5. (C) Respiratory rate and heart rate for the data shown in (A & B). Data is discontinuous during the baseline period, because accurate measurements could be made only when the mouse was resting quietly. Data points are continuous from the onset of the seizure, except for one data point during which breathing was obscured by movement artifact.

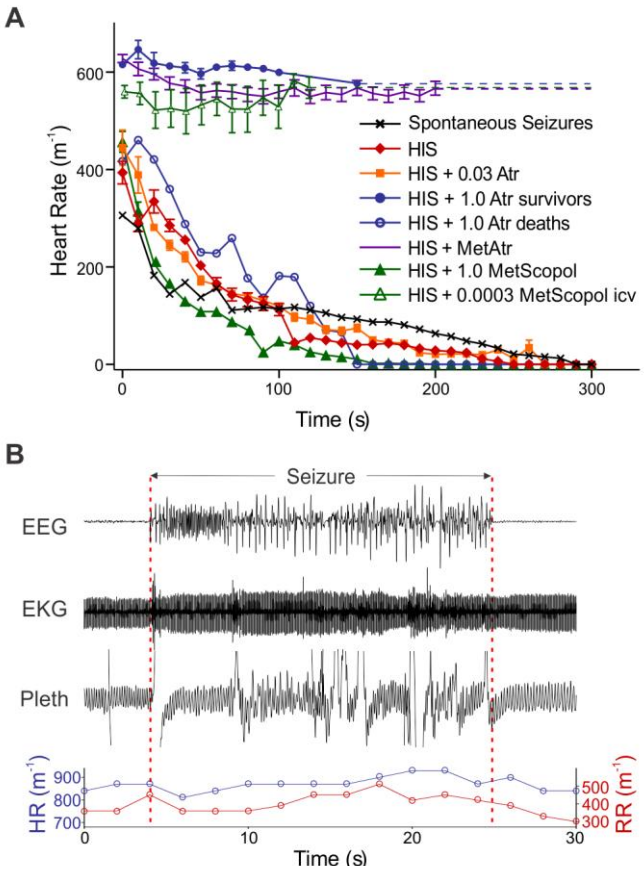

Figure 5. Postictal bradycardia is due to apnea, not increased parasympathetic drive. (A) Effect of muscarinic antagonists on postictal heart rate after heat-induced seizures (HIS). Untreated mice all died in response to heat-induced seizures (n=6). Atropine prevented bradycardia in 7/9 mice when given at a dose of 1 mg/kg (i.p.). Methylatropine (1 mg/kg; i.p.) also prevented bradycardia in 6/6 mice. Treatment with N-methylscopolamine given intracerebroventricularly at very low dose (0.3μg/kg) prevented bradycardia in all mice (n=5). In contrast, atropine (1 mg/kg; i.p.) did not prevent bradycardia or death in 2/9 mice, or when given at 0.03 mg/kg (n=6/6; i.p.), a dose selective for blockade of peripheral muscarinic receptors. Bradycardia also occurred after spontaneous seizures (n=2), and after pretreatment with N-methylscopolamine (1 mg/kg;i.p.; n=6/6). All mice with postictal bradycardiaalso had apnea, whereas apnea did not occur in any mouse without bradycardia. T=0 represents the time that apnea began. This was always during or at the end of seizures.Error bars are not shown for the two groups with n=2. (B) Heat-induced seizure in an *Scn1a*$^{R1407X/+}$mouse, 30 minutes after pre-treatment with atropine (1 mg/kg i.p.). During this seizure there was no apnea or bradycardia, and the mouse did not die.

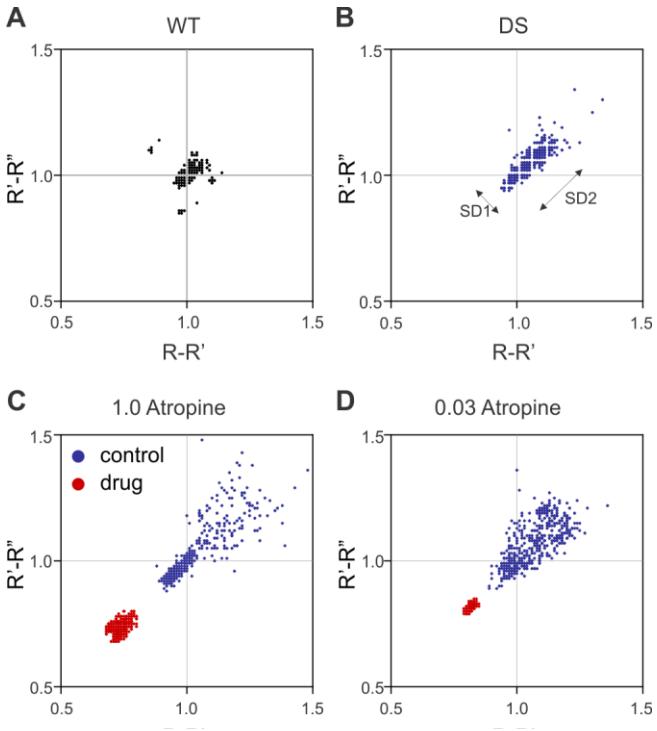

Figure 6. Low-dose and high-dose atropine were equally effective at blocking HRV. (A-B) Poincaré plots demonstrated greater short-term and long-term HRV (SD1 and SD2, respectively)in an *Scn1a*$^{R1407X/+}$mousecompared to a WT mouse. (C) High dose atropine (1 mg/kg) reduced HRV in an *Scn1a*$^{R1407X/+}$mouse, consistent with blockade of parasympathetic output. (D) Low dose atropine (0.03 mg/kg) was equally effective in reducing HRV in an *Scn1a*$^{R1407X/+}$mouse. The plots in the four parts of this Figure are from four individual animals. Summary data for replicate animals for these experiments are shown in Supplemental Figure 7. Number of replicates for each group was 7 (A), 10 (B), 6 (C) and 6 (D).

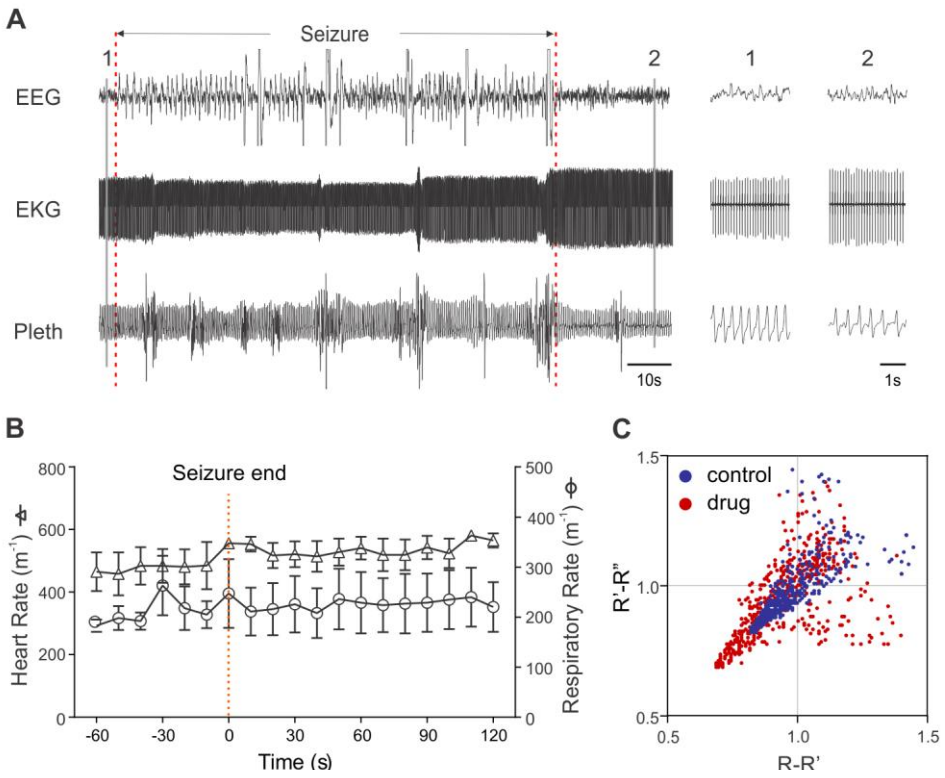

Figure 7. Peri-ictal apnea, bradycardia and death were prevented by N-methylscopolamine administered into the lateral cerebral ventricle at very low dose (0.0003mg/kg). (A) Heart rate and breathingdid not change in response to a heat-induced Racine scale 5 seizure in an *Scn1a*$^{R1407X/+}$mouse. Traces from top down are EEG, EKG and whole animal plethysmography. A seizure occurred at the time indicated. Insets to the right were obtained at the times indicated with the vertical lines on the left. Respiratory activity and the EKG did not change during the seizure. Note that there was movement artifact seen intermittently on the respiratory trace. Sudden changes in amplitude of the EKG were also an artifact due to movements of the animal. (B) Summary of results from *Scn1a*$^{R1407X/+}$mice with heat-induced Racine scale 5 seizures after N-methylscopolamine (0.3μg/kgi.c.v.; n=5). Breathing and heart rate were not affected in any of the mice. (C) Poincaré plots demonstrated that N-methylscopolamine (0.3μg/kgi.c.v.)did not block peripheral muscarinic receptors as seen by the lack of an effect on RR interval. The Poincaréplots shown here are from a single animal. Summary data for replicate animals for this experiment are shown in Supplemental Figure 7. Number of replicates was 4 animals.

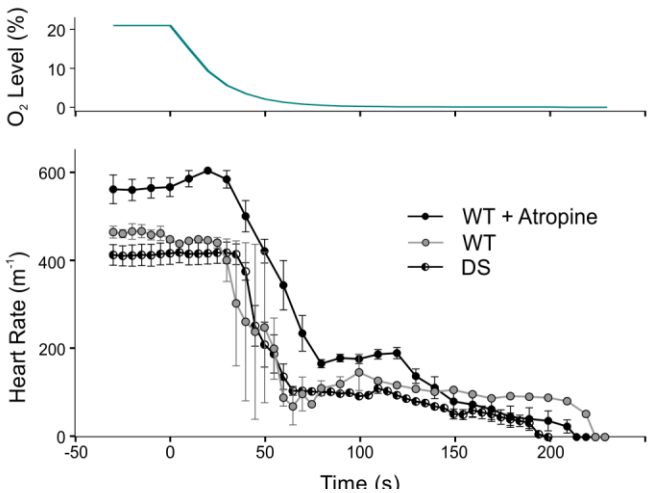

Figure 8. Anoxia caused bradycardia due to a direct effect on the heart. WT mice exposed to anoxia developed bradycardia (n=5). Pretreatment with atropine (1 mg/kg; i.p.) caused an increase in baseline heart rate, but did not prevent this bradycardia (n=5) indicating that bradycardia was not due to increased vagal output.*Scn1a*$^{R1407X/+}$ mice also developed bradycardia in response to anoxia (n=6).

Table

Table 1. Patients with Dravet Syndrome had abnormal breathing after seizures compared to localization-related epilepsy (p=0.018, Chi-square test).

		Dravet Syndrome	Localization-related epilepsy
Respiratory rhythm disturbance			
	Yes	4	0
	No	3	7
Loud postictal upper airway sounds*			
	Yes	1	3
	No	6	4

* noisy expiration, stertor, and grunting

Supplemental data

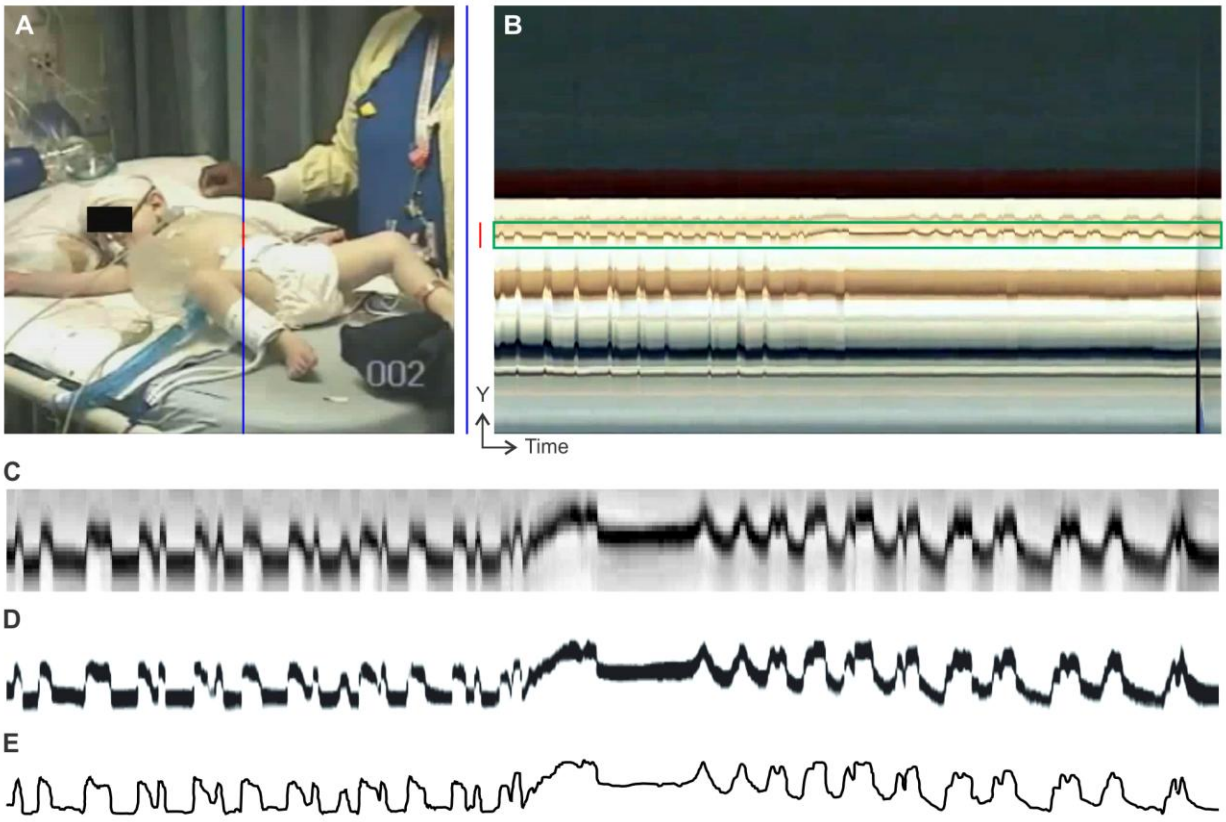

Supplemental Figure 1. Method used to analyze respiratory movements in videos of Dravet patients. (A) A region of interest was chosen from a frame of a video image (in this case a vertical line from Supplemental Video 1). This patient image is the same as that shown in Figure 1A. (B) A plot was generated with the y-axis representing the color values extracted for each pixel along the region of interest, and the x-axis representing successive video frames of the video (or time with video frame rate of 24 Hz). A band was then chosen where respiratory movements were maximized (in this case the box drawn around the umbilicus, which moved up and down with each breath). (C) Enlargement of the chosen band after conversion to grayscale image and contrast adjustment. (D) Movement of umbilicus clarified by cropping of surrounding image and conversion to black and white. (E) A line was drawn down the middle of the black region in D to obtain a line drawing of breathing movements.

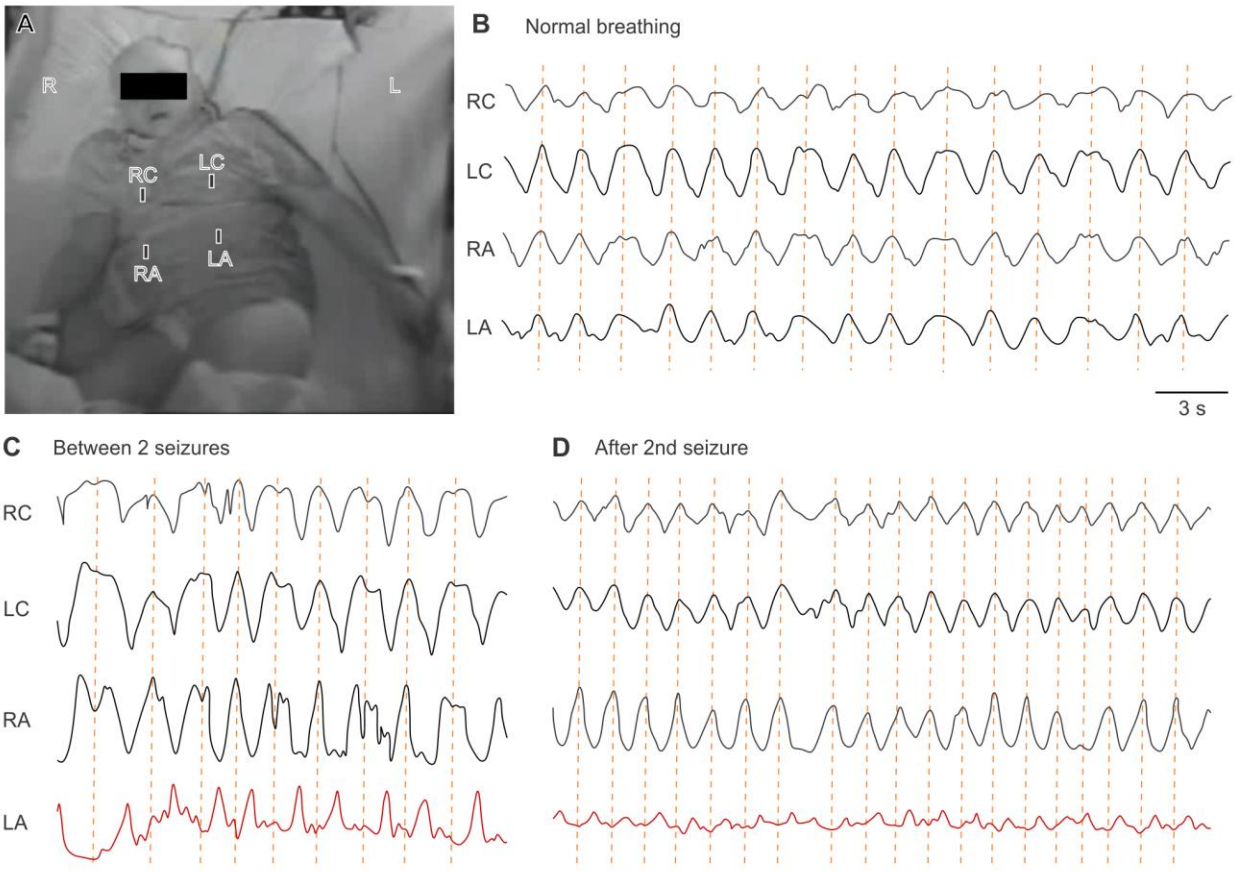

Supplemental Figure 2. Seizures induced paradoxical breathing in a DS patient. (A) Video frame illustrating four separate regions of interest for analysis of respiratory movements. (B) Normal breathing movements from the four regions of interest. Analysis was performed as illustrated in Supplemental Figure 1, except that a single line was used to illustrate breathing movement for each region of interest. Note that breathing occurs in phase for each quadrant of the torso (vertical dashed lines). (C) Breathing between two convulsive seizures. Note that breathing is irregular and erratic, and that movements at LA are 180 degrees out of phase with the other three quadrants. (D) Breathing after second convulsive seizure. Note that the LA movements are now much smaller and remain out of phase. RC & LC – Right and left chest. RA & LA – Right and left abdomen. The video of this patient can be played from Supplemental Video 2.

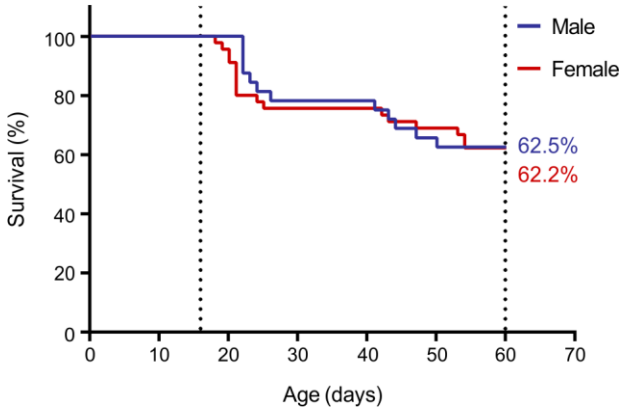

Supplemental Figure 3. Survival curves for male (n=32) and female (n=45)*Scn1a*$^{R1407X/+}$ mice. Methods are the same as those used for Figure 3. There was no gender difference in survival(p=0.871; Log-rank Mantel-Cox test)

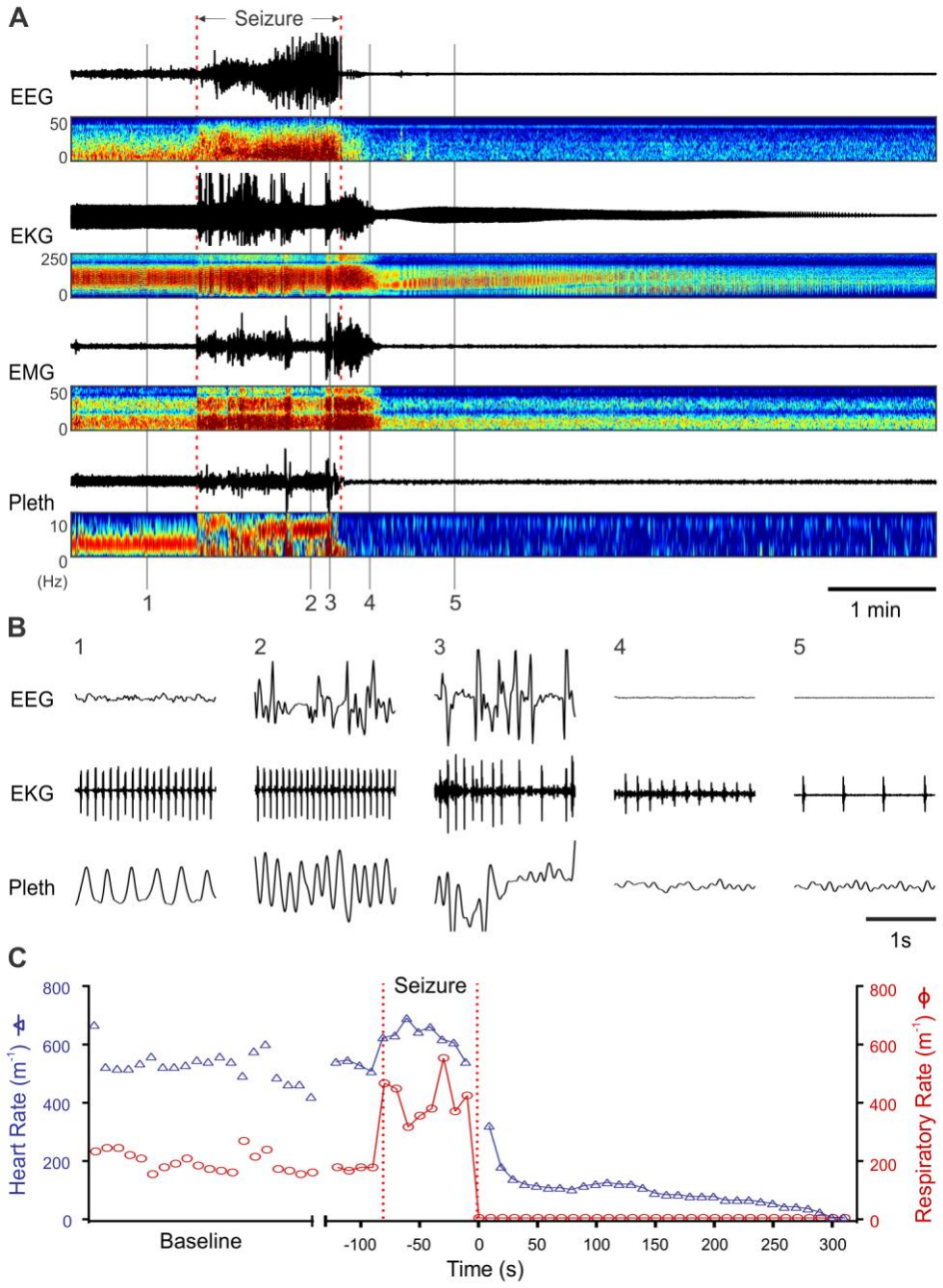

Supplemental Figure 4. Postictal death after a spontaneous seizure in a 2nd *Scn1a*$^{R1407X/+}$ mouse(P24). (A) Physiological recordings with corresponding power spectrum heat maps (using same format as Figure 4) showing events leading to death. Breathing became disrupted during the seizure and ceased at the end of the seizure. In contrast, bradycardia began later and terminal asystole did not occur until nearly 5 minutes after the end of the seizure. (B) Expanded traces of EEG, EKG and plethysmography from times marked by vertical lines labelled in A as 1-5. (C) Plot of breathing and heart rate for the data in A.

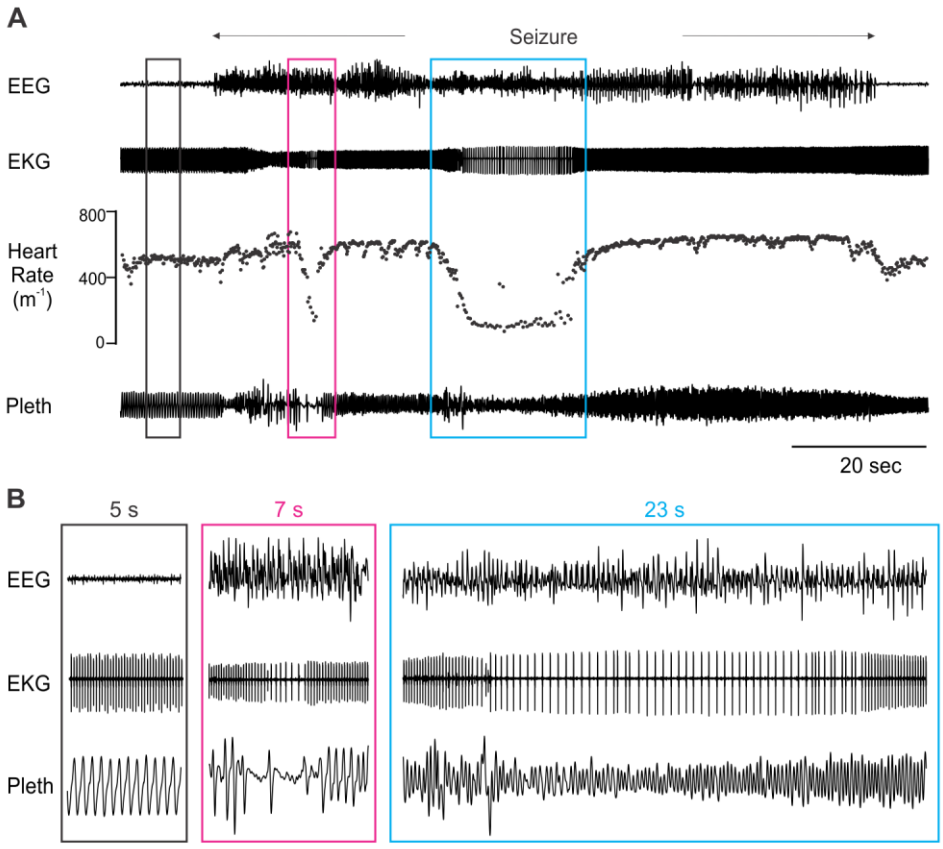

Supplemental Figure 5. Spontaneous non-fatal seizure in an *Scn1a*$^{R1407X/+}$mousethat died 5.5 hours later from a spontaneous seizure. (A) Physiological recordings duringa spontaneous non-fatal seizure showing EEG, EKG instantaneous heart rate and plethysmography. This non-fatal seizure was associated with disruption of breathing, including apnea. During the second, longer episode breathing frequency was increased but tidal volume was greatly decreased. During both episodes bradycardia also occurred, but followed the onset of abnormal breathing. The apnea and bradycardia were both less severe than during the fatal seizure that occurred later. This is the same mouse as that shown in Figure 4. (B) Expanded traces from times designated in A by the colored boxes.

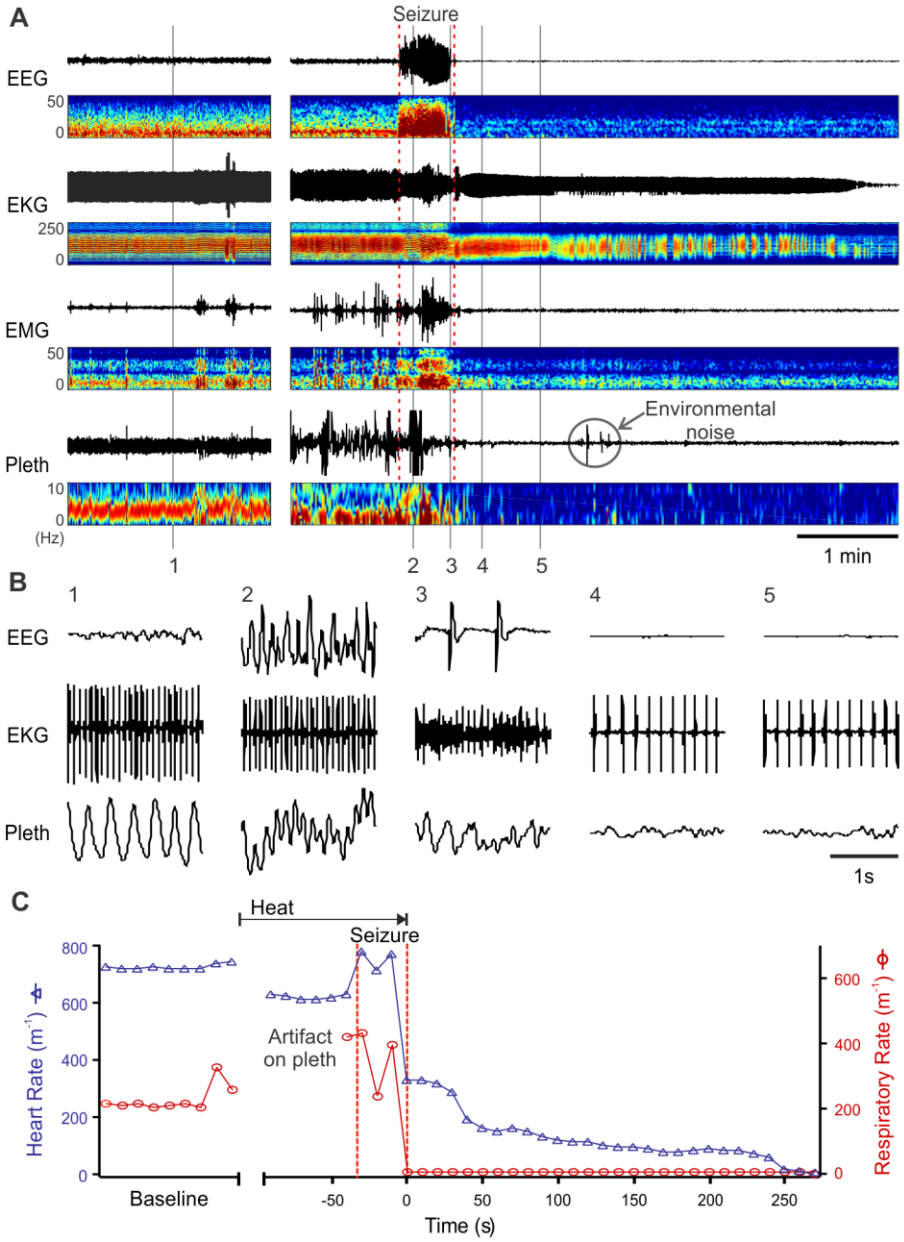

Supplemental Figure 6. Death of *Scn1a*$^{R1407X/+}$ mice after heat-induced seizures was also due to respiratory arrest followed by bradycardia. (A) Events leading to death of a mouse during a heat-induced seizure. Data are shown in same format as in Figure 4. Traces are discontinuous to show baseline recordings prior to hyperthermia. At the time indicated, a seizure occurred after the animal's temperature had increased to 38.9 degrees C. After the seizure, PGES was seen on the EEG. Towards the end of the seizure, breathing became erratic, and then respiratory activity suddenly ceased. The EKG showed a rapid decrease in heart rate at the end of the seizure, after which the frequency and amplitude slowly decreased over the next four minutes. (B) Expanded traces of EEG, EKG and plethysmography at the times labelled 1-5. (C) Respiratory rate and heart rate for the data shown in A & B. Data points are discontinuous prior to the seizure due to movement artifact.

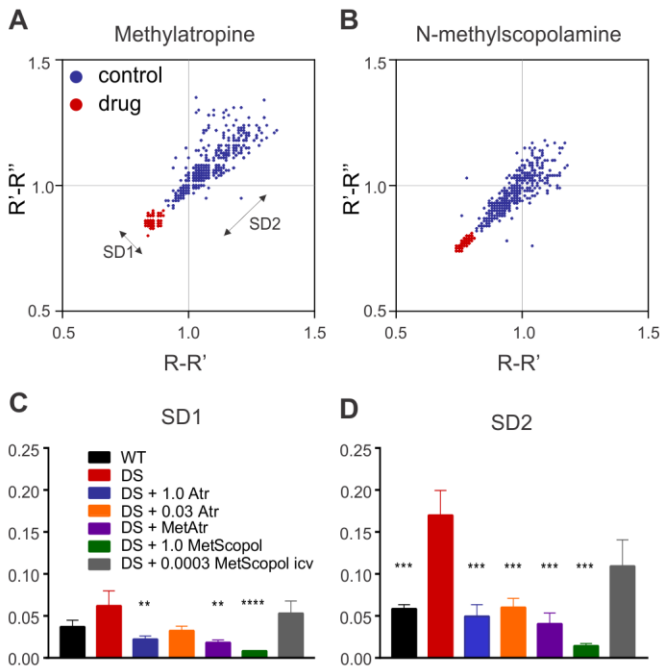

Supplemental Figure 7. Effect of atropine and quaternary ammonium derivatives on HRV. (A-B) Poincaré plots demonstrate that methylatropine (1 mg/kg) and N-methylscopolamine (1 mg/kg) both reduced HRV in *Scn1a*$^{R1407X/+}$mice. The plots in parts A & B are from two individual animals. Summary data for replicate animals for these experiments are shown in parts C & D. Number of replicates was 6 for part A and 7 for part B. (C) Short-term HRV for each group from panels A-B, Figure 6and Figure 7. (D) Long-term HRV for each group from panels A-B, Figure 6and Figure 7. Number of animals for each experiment are (for bars from right to left): 7, 10, 6, 6, 6, 7, 4. Symbols represent p-values compared to DS group (Mann-Whitney U Test). * - $p<0.01$; ** - $p<0.001$; *** - $p<0.0001$.

Supplemental Video 1. Video of a Dravet Syndrome patient during and after a seizure. Panel on left is the original video. Panel on right was processed with phase-based Eulerian video magnification motion processing to enhance respiratory movements (4X; 0.05-3 Hz).

Supplemental Video 2. Video of a second Dravet Syndrome patient during and after a seizure. Video was processed with Eulerian video magnification to enhance respiratory movements (10X; 0.05-3 Hz).